INTERNATIONAL ATOMIC ENERGY AGENCY
UNITED NATIONS EDUCATIONAL, SCIENTIFIC AND CULTURAL ORGANIZATION
INTERNATIONAL CENTRE FOR THEORETICAL PHYSICS
I.C.T.P., P.O. BOX 586, 34100 TRIESTE, ITALY, CABLE: CENTRATOM TRIESTE

H4.SMR/845-5

Second Winter College on Optics

20 February - 10 March 1995

Fourier Optics and Optical Information Processing

J.C. Dainty

Imperial College of Science and Technology
The Blackett Laboratory
London, United Kingdom

COURSE K

CONTENTS

INTRODUCTION

These notes have been prepared for a half-day course in Optical Information Processing as part of the Applied Optics Summer Course given at Imperial College in July 1985. My aim has been to give the basic principles of various techniques of analysing data using optical systems. References to specific topics are given in each Section, although no attempt has been made to be complete in this respect. For further reading I would suggest the following books:

R N Bracewell, 'The Fourier Transform and its Applications'. McGraw Hill, 2nd Ed 1978

D Casasent (Editor) ,'Optical Data Processing: Applications', Topics in Appl Phys 23, Springer Verlag, 1978

J W Goodman, 'Introduction to Fourier Optics', McGraw Hill, 1968

S H Lee (Editor), 'Optical Information Processing', Topics in Appl Phys 48, Springer-Verlag, 1981

G L Rogers, 'Noncoherent Optical Processing', Wiley 1977

H Stark (Editor), 'Applications of Optical Fourier Transforms', Academic Press, 1982

F T S Yu, 'Optical Information Processing', Wiley 1982

An excellent review of modern developments is given by Goodman in IE and IREE Aust., 2, 139-149 (1982).

1. FOURIER TRANSFORMS

1.1 One and Two Dimensional Fourier Transforms

Let f(x) represent some physical quantity of interest, for example the complex amplitude of light as a function of distance across a slit. The Fourier transform of f(x) is defined as

$$F(u) = \int_{-\infty}^{\infty} f(x) \exp(-2\pi i u x)\, dx \qquad (1.1)$$

The units of the variable u are reciprocal to those of x - thus if x has units of length, u has units of inverse length or spatial frequency.

The function F(u) is called the Fourier transform of f(x). It contains all of the information present in f(x), but displays that information in a different way (i.e. as a function of u instead of x). The original function f(x) can be obtained from F(u) by an inverse Fourier transform:

$$f(x) = \int_{-\infty}^{\infty} F(u) \exp(2\pi i u x)\, du \qquad (1.2)$$

As an example, consider the function, called rect (x/a), that could represent the complex amplitude of light across a slit,

$$\begin{aligned} \text{rect } (x/a) &= 1 \qquad |x| < a/2 \\ &= 0 \qquad |x| > a/2 \end{aligned}$$

This function is shown in Fig 1.1(a). Its Fourier transform is

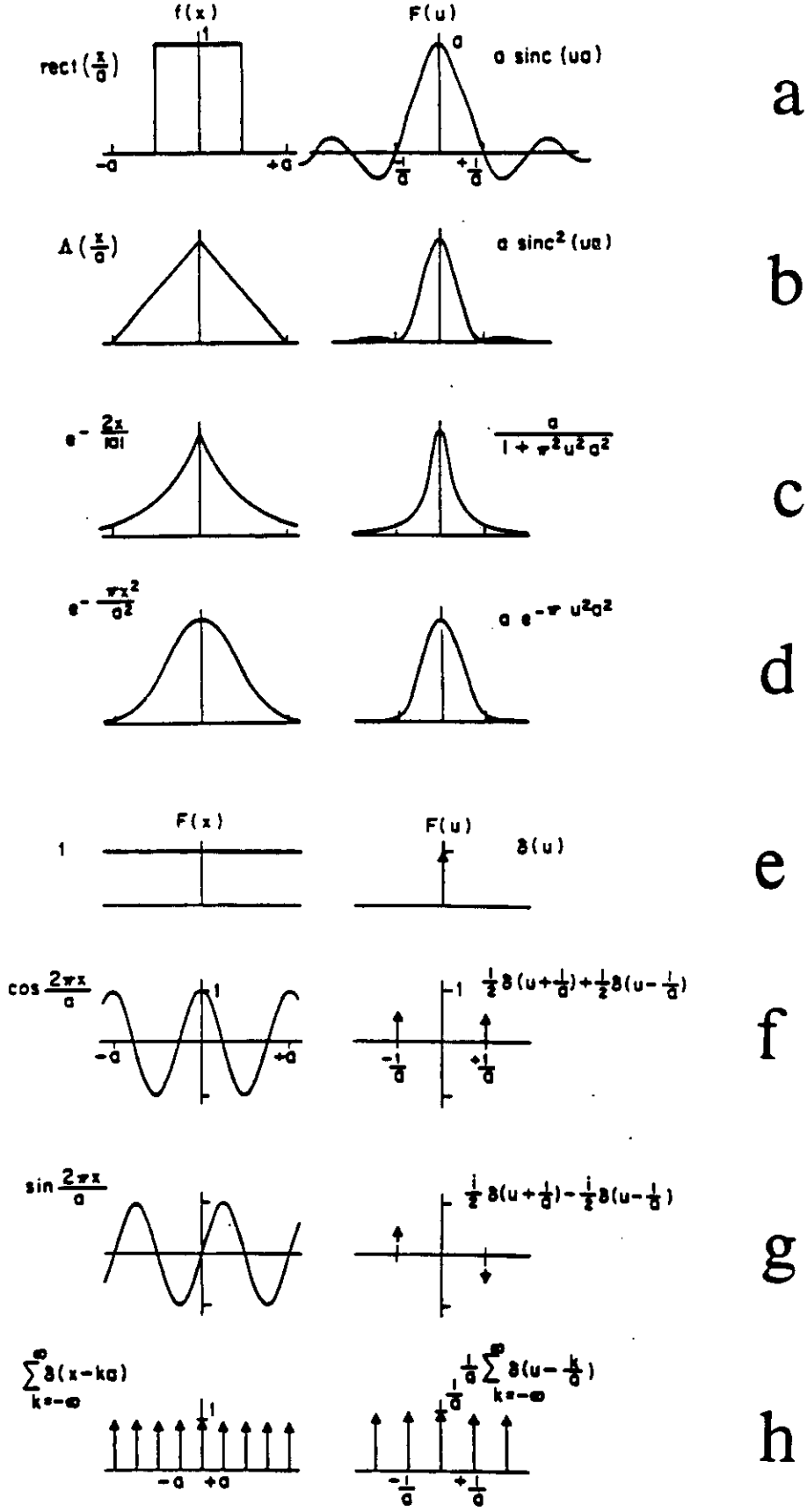

Figure 1.1 Some one-dimensional Fourier transform pairs

$$F(u) = \int_{-\infty}^{\infty} f(x)\, \exp(-2\pi i u x)\, dx$$

$$= \int_{-a/2}^{a/2} \exp(-2\pi i u x)\, dx$$

$$= \left[\frac{\exp(-2\pi i u x)}{-2\pi i u} \right]_{-a/2}^{a/2}$$

$$= \frac{\sin(\pi u a)}{\pi u}$$

or,

$$F(u) = a\, \mathrm{sinc}(ua) \ ,$$

where $\mathrm{sinc}(X) = \sin(\pi X)/(\pi X)$.

Other examples of one dimensional Fourier transforms are shown in Fig 1.1.

The two dimensional Fourier transform is defined in a similar way:

$$F(u,v) = \iint_{-\infty}^{\infty} f(x,y)\, \exp[-2\pi i(ux+vy)]\, dx\, dy \qquad (1.3)$$

and the inverse Fourier transform is

$$f(x,y) = \iint_{-\infty}^{\infty} F(u,v)\, \exp[+2\pi i(ux+vy)]\, du\, dv \qquad (1.4)$$

Figure 1.2 illustrates the meaning of a two dimensional spatial frequency - it is simply a one dimensional sinusoidal sheet of frequency $w = (u^2 + u^2)^{1/2}$ at an angle $\theta = \tan^{-1}(v/u)$ to the u-axis. Figure 1.3 shows some two dimensional Fourier transform pairs.

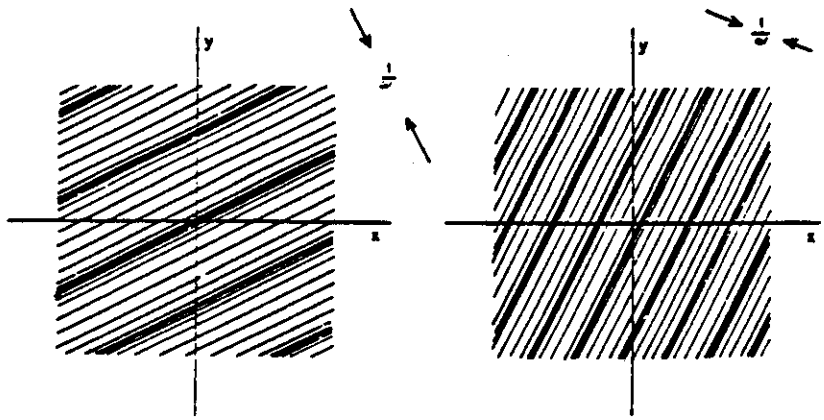

Figure 1.2 Two-dimensional spatial frequencies

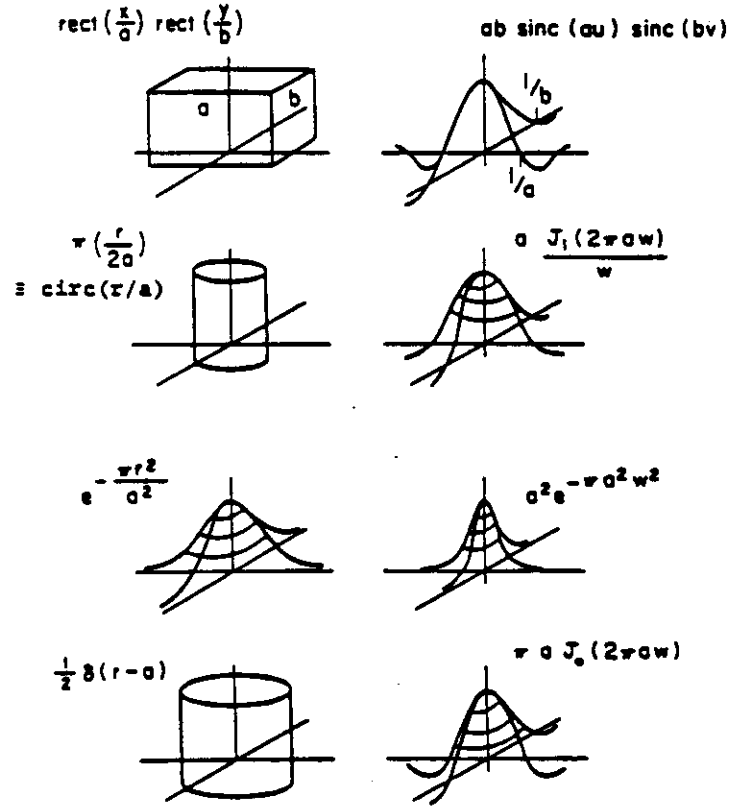

Figure 1.3 Some two dimensional Fourier transform pairs

1.2 Convolution and Correlation

The convolution of two functions f(x) and g(x) yields a third function h(x) defined by

$$h(x') = \int_{-\infty}^{\infty} f(x)\, g(x'-x)\, dx \qquad (1.5)$$

Convolution is often denoted by the symbol *:

$$h(x) = f(x) * g(x) \quad .$$

Figure 1.4 illustrates the convolution of two functions.

In two dimensions, convolution is defined by

$$h(x',y') = \iint_{-\infty}^{\infty} f(x,y)\, g(x'-x,y'-y)\, dx\, dy \quad . \qquad (1.6)$$

The process of convolution occurs often in optical systems. For example, when imaging in spatially incoherent light with an isoplanatic optical system, the image intensity i(x,y) is equal to the convolution of the object intensity o(x,y) with the point spread function p(x,y):

$$i(x,y) = o(x,y) * p(x,y) \quad . \qquad (1.7)$$

In this case (and in many other similar cases), we may know i(x,y) (the image intensity) and p(x,y) (the point spread function) and wish to find the object intensity o(x,y). This is not a straightforward problem if we consider only the (x,y) space. By using Fourier transforms, however, the problem is quite easy, at least in the absence of noise.

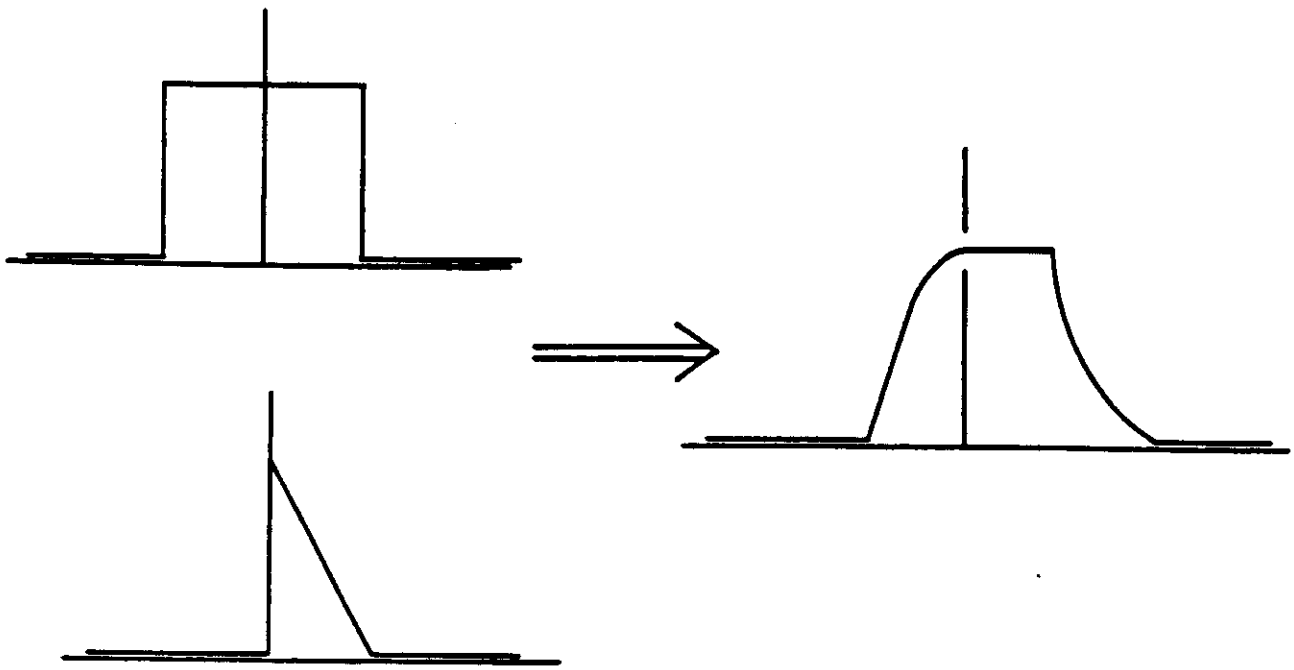

Figure 1.4 The convolution of two real functions

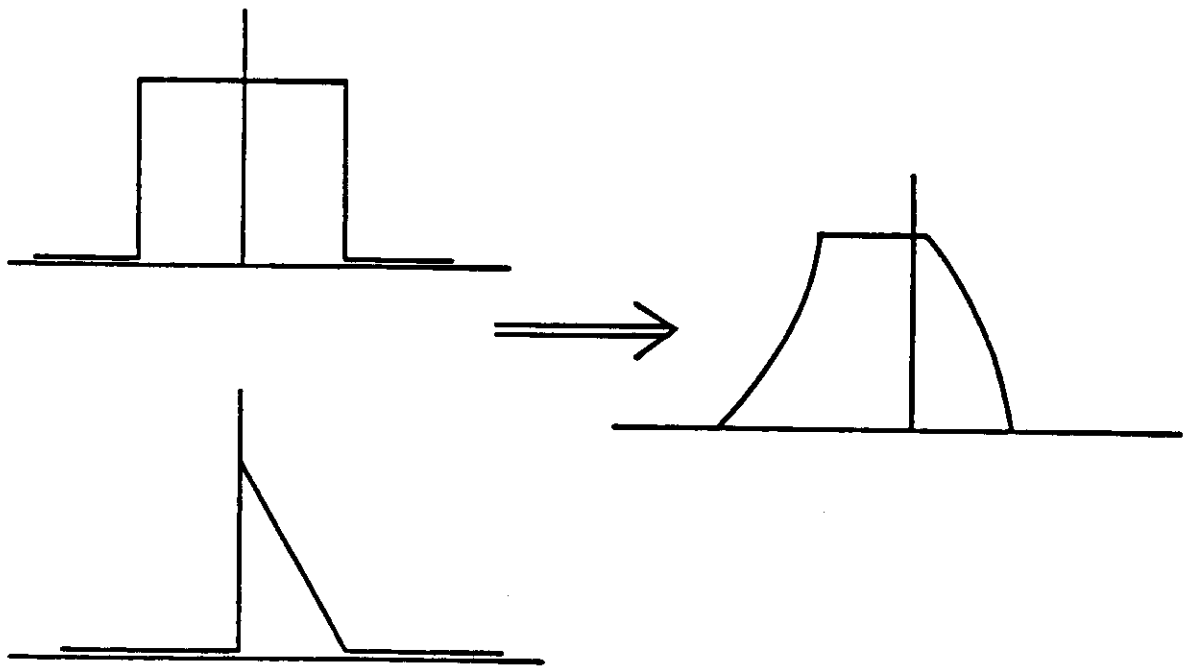

Figure 1.5 The cross-correlation of two real functions

The convolution theorem states that the Fourier transform of a convolution equals the product of the Fourier transforms. That is, if

$$h(x) = f(x) * g(x) ,$$

then

$$H(u) = F(u)\, G(u) \qquad (1.8)$$

Thus, to solve for the object intensity in (1.7), we (i) find the Fourier transforms I(u,v) and P(u,v) of i(x,y) and p(x,y) respectively, (ii) divide, yielding O(u,v) = I(u,v)/P(u,v), and (iii) find the inverse Fourier transform of O(u,v). This may seem at first sight to be a complicated procedure, but it is readily carried out either by a digital computer or by a suitable coherent optical system (see Section 4).

The cross-correlation of two functions is defined in one dimension by

$$h(x') = \int_{-\infty}^{\infty} f^*(x)\, g(x'+x)\, dx \qquad (1.9)$$

and in two dimensions by

$$h(x',y') = \iint_{-\infty}^{\infty} f^*(x,y)\, g(x'+x,y'+y)\, dx\, dy \qquad (1.10)$$

Cross-correlation is illustrated in Figure 1.5. It is very similar, but not identical to convolution. Finally the two dimensional spatial autocorrelation function is defined by

$$h(x',y') = \iint_{-\infty}^{\infty} f^*(x,y)\, f(x'+x,y'+y)\, dx\, dy . \qquad (1.11)$$

1.3 Sampling Theorem

This states that

'A function whose Fourier transform is zero for $|u| > u_{max}$ (i.e. a bandlimited function) is fully specified by values spaced at intervals $\delta x < 1/(2u_{max})$, except for any harmonic term with zeros at the sampling points.'

This is an extremely important theorem in practice, because it tells us how to sample continuous functions without losing any information.

Let $f(n\delta x)$, $n = -\infty \ldots\ldots + \infty$, be samples of $f(x)$ taken at intervals δx. The samples $f(n\delta x)$ can be used to reconstruct the continuous function $f(x)$ using the following interpolation formula:

$$f(x) = \{ \sum_{-\infty}^{\infty} f(n\delta x)\, \delta(x-n\delta x) \} * \mathrm{sinc}(x/\delta x) , \qquad (1.12)$$

where $\delta(\ )$ is the delta function. Figure 1.6 illustrates the sampling theorem.

The best textbook for further reading on Fourier transforms is by R N Bracewell, 'The Fourier Transform and its Applications', 2nd Ed, McGraw Hill, 1978.

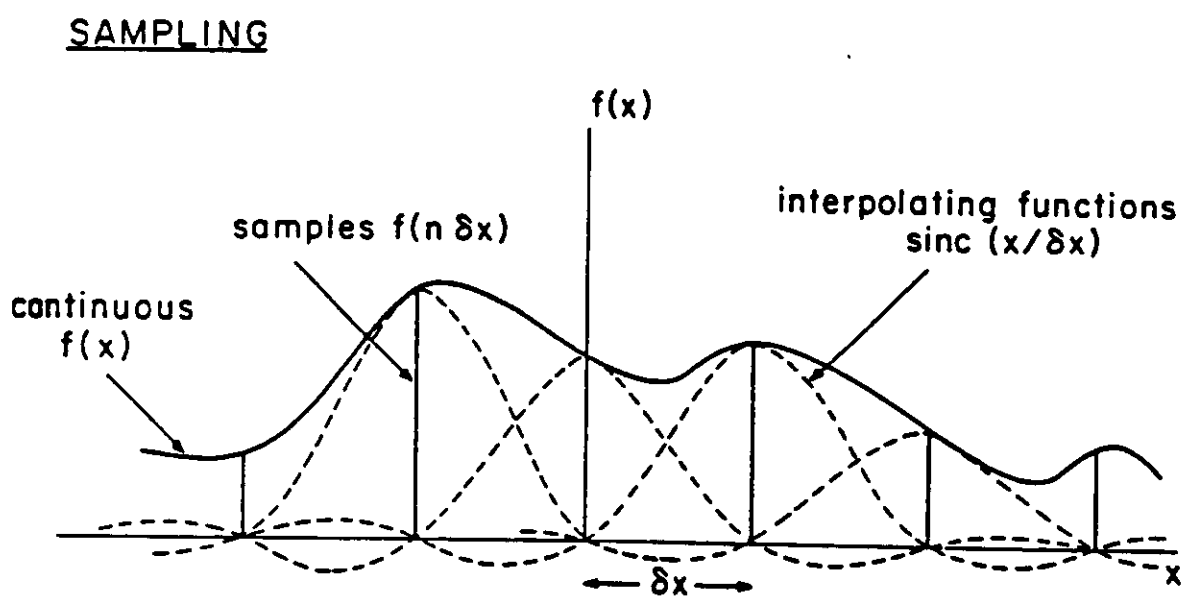

Figure 1.6 Illustration of the reconstruction of a continuous function f(x) from samples f(nδx) of it (see Eq.1.12)

2. FOURIER TRANSFORMING PROPERTIES OF LENSES

2.1 Fraunhofer Diffraction Formula

Suppose that some distribution of complex amplitude $U(\xi,\eta)$ fills an aperture - if the light diffracted by the aperture is viewed at a large distance z, then the complex amplitude in the observation plane $U(x,y)$ is given by the Fraunhofer diffraction formula:

$$U(x,y) = \frac{-i}{\lambda}\frac{\exp(ikz)}{z}\exp\left[\frac{ik(x^2+y^2)}{2z}\right] \iint_{-\infty}^{\infty} U(\xi,\eta)\exp\left[\frac{-2\pi i}{\lambda z}(x\xi+y\eta)\right] d\xi\, d\eta \qquad (2.1)$$

Eq.(2.1) applies when the distance from the (ξ,η) plane to the (x,y) is large ($z \to \infty$) or effectively large. The important thing is that light diffracted at a certain angle corresponds to a particular point in the (x,y) plane. This can be achieved with a well-corrected lens, as shown in Fig 2.1. Thus the Fraunhofer diffraction formula (2.1) relates the complex amplitude at the focus of a well-corrected lens to that in the pupil of the lens.

Consider the arrangement shown in Fig 2.2 in which a transparency of complex amplitude transmittance $t(\xi,\eta)$ is illuminated by a plane wave. In this case, $U(\xi,\eta) = t(\xi,\eta)$ and Eq.(2.1) may be written

$$U(x,y) = \frac{-i}{\lambda}\frac{\exp(ikz)}{z}\exp\left[\frac{ik(x^2+y^2)}{2z}\right] T\left(\frac{x}{\lambda z},\frac{y}{\lambda z}\right) , \qquad (2.2)$$

where $T(x/\lambda z,\ y/\lambda z)$ is the Fourier transform of the transmittance $t(\xi,\eta)$ of the transparency. Note that this Fourier transform is evaluated at spatial frequencies $(u,v) = (x/\lambda z,\ y/\lambda z)$ - that is, distances (x,y) in the observation plane are equivalent to spatial frequencies (u,v) of the object. We relate these quantities using the

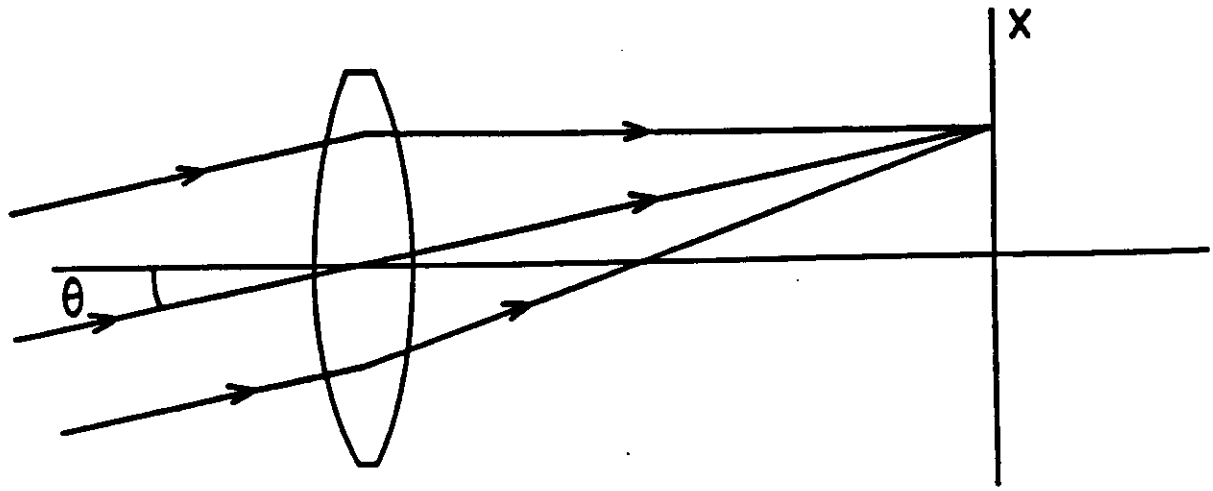

Figure 2.1 Use of a lens to focus parallel rays

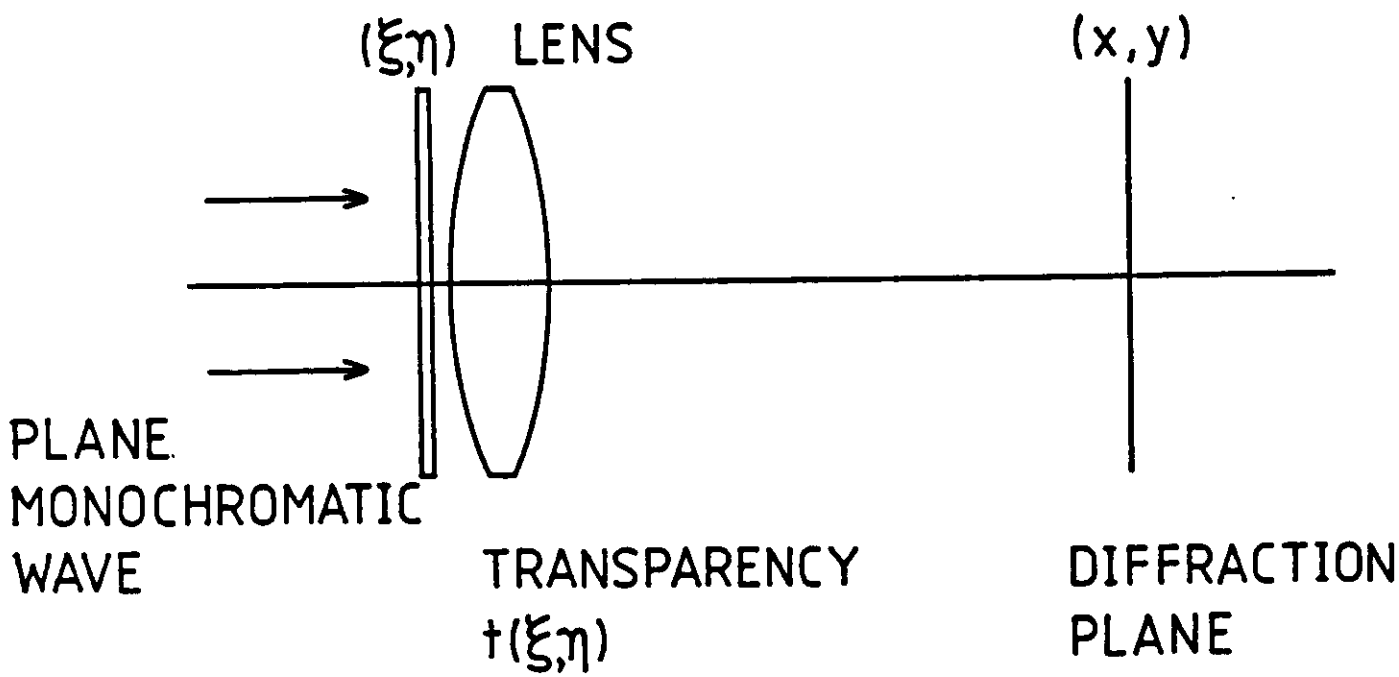

Figure 2.2 The use of a lens to form a Fraunhofer diffraction pattern

factor λz:

$$x = \lambda z u \quad , \quad y = \lambda z v$$
$$u = x/\lambda z \quad , \quad v = y/\lambda z \qquad (2.3)$$

Equation (2.2) shows that the complex amplitude U(x,y) in the plane of focus is closely related to the Fourier transform of $t(\xi,\eta)$, but not equal to it. If one is only interested in the <u>intensity</u> in the observation plane, then the phase factors in Eq.(2.2) disappear leaving

$$I(x,y) = \frac{1}{(\lambda z)^2} \left| T\left(\frac{x}{\lambda z}, \frac{y}{\lambda z}\right) \right|^2 . \qquad (2.4)$$

Thus, apart from the unimportant constant $1/(\lambda z)^2$, the intensity at the focal plane equals the <u>squared modulus</u> of the Fourier transform of the complex amplitude transmittance. This is the basis of the technique of <u>diffraction pattern sampling</u> described in Section 3.

2.2 Exact Fourier Transform

In Eq.(2.2), the first two factors

$$\frac{-i}{\lambda} \frac{\exp(ikz)}{z} ,$$

do not depend on (x,y) and can usually be neglected, leaving

$$U(x,y) = K \exp\left[\frac{ik(x^2+y^2)}{2z}\right] T\left(\frac{x}{\lambda z}, \frac{y}{\lambda z}\right) , \qquad (2.5)$$

where K is the unimportant (complex) constant.

The remaining phase factor exp [ ] represents, in physical terms, a

spherical wave centered in the diffracting pupil and its presence prevents the existence of an exact Fourier transform of $t(\xi,\eta)$ in the observation plane.

It can be shown that this phase factor can be cancelled by an equal and opposite factor if the transparency $t(\xi,\eta)$ is placed in the front focal plane of the lens, as shown in Fig 2.3. In this case,

$$U(x,y) = K\ T\left(\frac{x}{\lambda f},\frac{y}{\lambda f}\right) \qquad (2.6)$$

where the distance z has been replaced by the focal length f. This is an important result, for it signifies that the optical arrangement shown in Fig 2.3 can be used to perform an exact Fourier transform - this arrangement is in fact the building block of many coherent optical processors.

The detailed design of lenses for Fourier transforming optical systems is discussed by van Bieren, Appl Optics, 10, 2739-2742 (1971). For further reading on the Fourier transforming properties of lenses, see J W Goodman, 'An Introduction to Fourier Optics', McGraw-Hill, 1968.

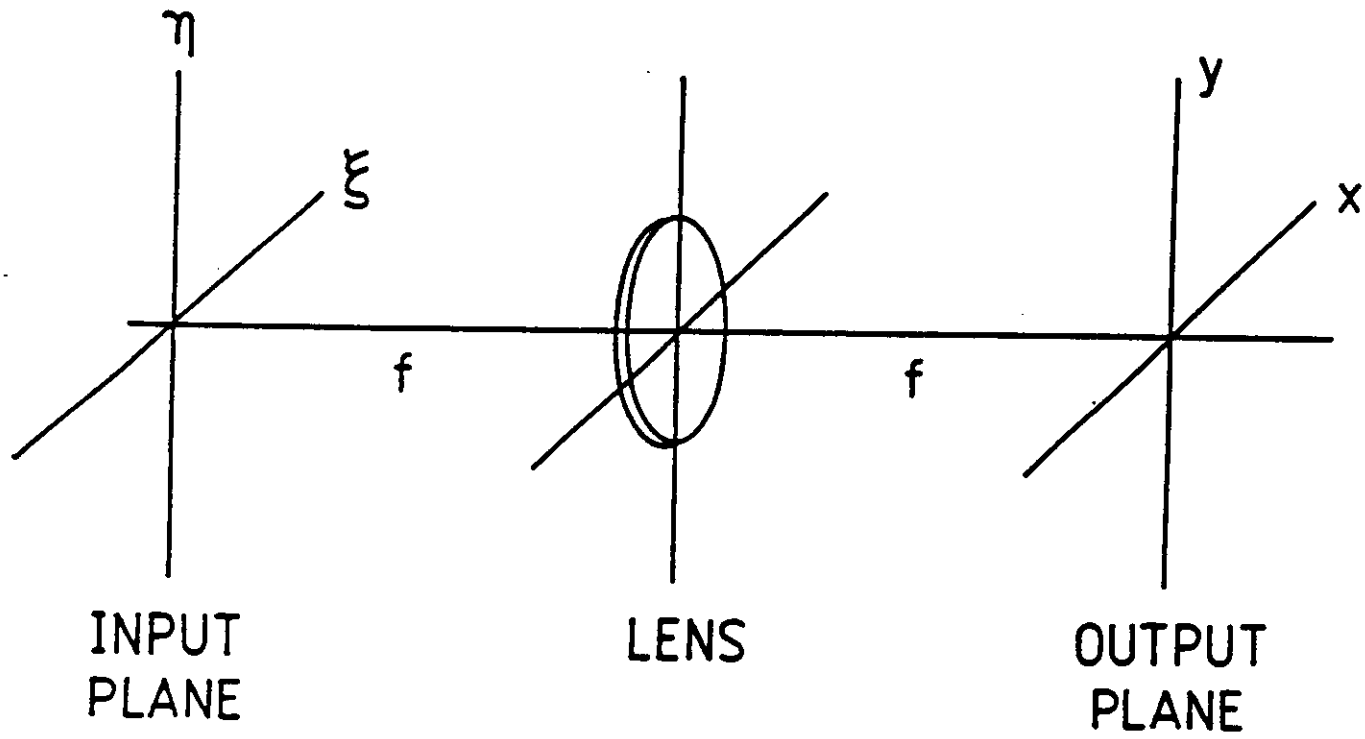

Figure 2.3 The building block for a coherent optical processor. The complex amplitude U(x,y) in the back focal plane of the lens is proportional to the Fourier transform of the amplitude U(ξ,η) in the front focal plane.

3. DIFFRACTION PATTERN SAMPLING

This is the simplest and probably the most successful application in commercial terms of coherent optical processing. The intensity of a Fraunhofer diffraction pattern (i.e. the squared modulus of the Fourier transform) of an object is measured using a suitable detector, usually linked to a computer, with the aim of estimating some parameter of the object such as its size or shape.

Most of the commercial applications have the aim of measuring size of known shapes of objects, e.g. particle size distribution and wire/fibre diameters, and the discussion below is directed particularly at the measurement of droplet sizes in aerosols. In some scientific applications, the diffraction pattern intensity itself is of interest and its measurement provides structural information about the diffracting screen (such as a transparency).

The basic optical arrangement is similar to Fig 2.2 and is shown with some possible detection methods in Fig 3.1. In this arrangement, distances (x,y) in the Fourier plane are related to spatial frequencies (u,v) of the object by

$$x = \lambda f u \quad , \qquad y = \lambda f v \quad ,$$

where λ is the optical wavelength and f is the focal length of the lens. Note that the distance from the diffracting object to the lens does not enter into this relationship, with the result that a measurement of the size of an object does not depend on its location in the diffracting volume. This fact allows the technique to be applied to the measurement of particle size distributions in a volume.

In order to understand the basic principles of diffraction pattern sampling, consider first the estimation of the diameter of a round hole in an opaque screen. The diffraction pattern intensity (squared modulus of Fourier transform) is given by (see Fig 1.3):

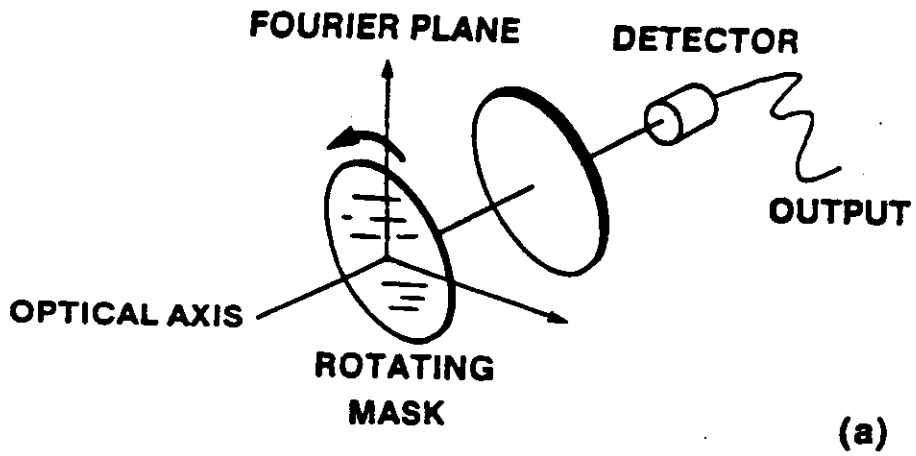

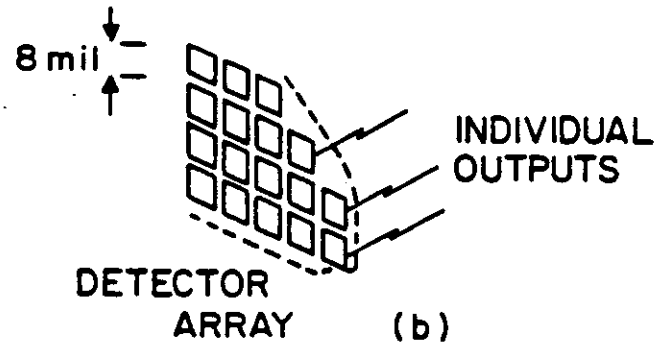

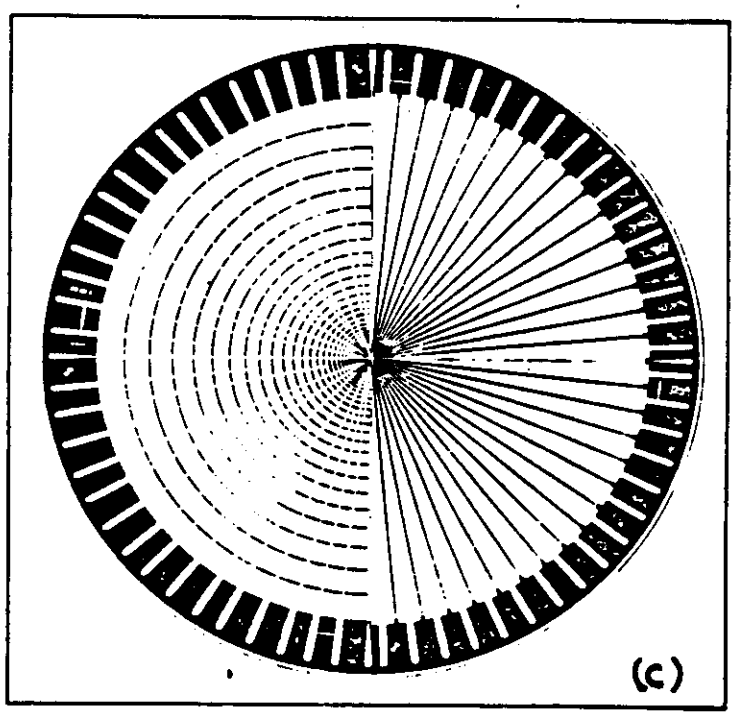

Figure 3.1 Upper: optical system for diffraction pattern sampling. Lower: three possible detector types, (a) rotating mesh (b) diode array (c) ring-wedge detector. (After B J Thompson, 'Coherent Optics', Univ. Rochester Summer School Notes)

$$I(r) = \left[\frac{2J_1(\frac{\pi dr}{\lambda f})}{(\frac{\pi dr}{\lambda f})} \right]^2 , \qquad (3.1)$$

where r is a radial coordinate ($r^2 = x^2 + y^2$), and d is the diameter of the hole. A photograph of this intensity is shown in Fig 3.2 along with a graph of I(r) v r: this function is called the Airy disc function and the radius of the first dark ring is given by

$$r_{min} \sim 1.22\lambda f/d \ . \qquad (3.2)$$

Thus a simple measurement of r_{min} yields the diameter d if λ and f are known. For example, if λ = 633 nm and f = 200 mm, a measured radius of the first dark ring of 5.0 mm yields a pinhole diameter equal to $d \sim 1.22\lambda f/r_{min}$ = 31 μm. Note that the <u>smaller</u> the hole, the <u>larger</u> the diffraction pattern.

The extension of the technique to the measurement of particle or droplet size distributions in a volume is non-trivial. First one assumes that Babinet's Principle holds: that is, if the diffraction amplitudes produced by no screen, a certain screen and its complement are U_1, U_2 and U_3 respectively, then $U_1 = U_2 + U_3$. Thus at any point where $U_1 = 0$, if follows that $U_1 = -U_2$ and $I_1 = I_2$.

The complement of a pinhole is an opaque disc. Real particles or droplets are not opaque discs and some assumption regarding their shape and/or refracting properties may be necessary. For very small particles, scalar diffraction theory is not applicable and it may be necessary to use Mie scattering theory. Finally, when there is a <u>distribution</u> of sizes, the inverse problem of estimating the histogram of particle sizes from the diffraction pattern intensity is not straightforward. Further information on the inverse problem is given by W L Anderson in the review book by Stark (see Introduction).

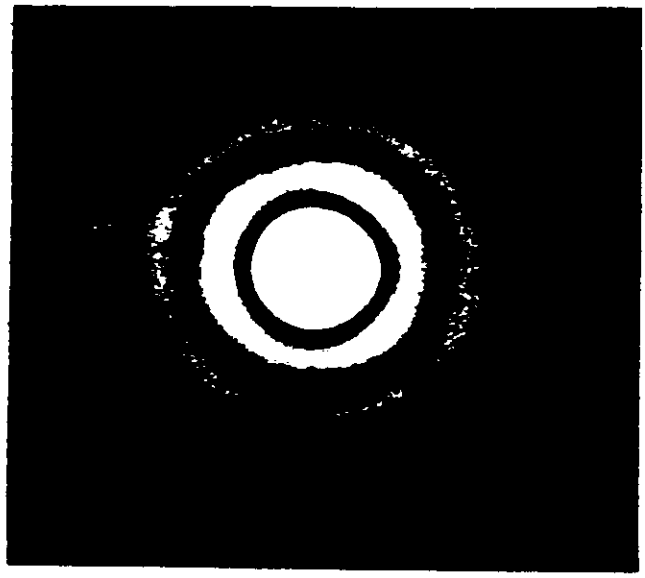

x	$\left[2\frac{J_1(\pi x)}{\pi x}\right]^2$	max or min
0	1	max
1.220	0	min
1.635	0.0175	max
2.233	0	min
2.679	0.0042	max
3.238	0	min
3.699	0.0016	max

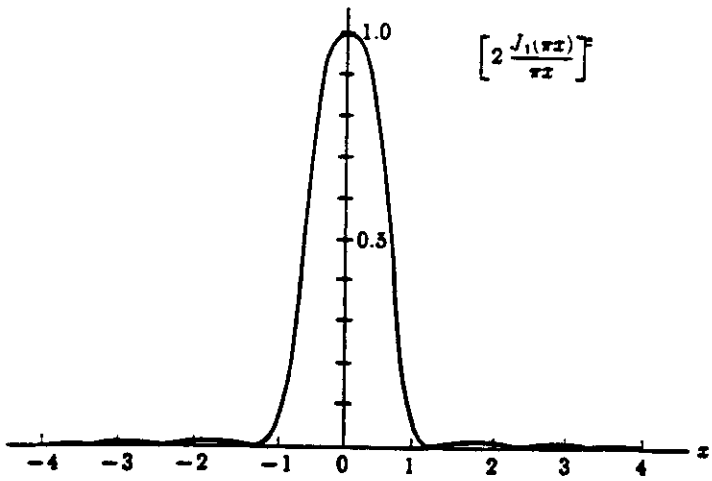

Figure 3.2 The diffraction pattern intensity produced by a circular hole of diameter d: this is called the Airy disc function. The first zero of intensity occurs at a value of r equal to $1.22\lambda f/d$

4. COHERENT OPTICAL PROCESSOR

4.1 Optical Layout

The most common layout for a coherent optical processor is shown in Fig 4.1. A laser beam is sent through a beam expander, pinhole spatial filter and collimating lens to produce a uniform plane wave. This is incident on a transparency (or other input device, see Section 8) of amplitude transmittance $t(\xi,\eta)$ to yield a complex amplitude $U_1(\xi,\eta) = t(\xi,\eta)$ in the input plane of the processor. The input plane (1), first lens, spatial frequency plane (2), second lens and output plane (3) are each separated by the focal length f of the (identical) lenses. Thus, according to the analysis in Section 2, the complex amplitude $U_2(x,y)$ in plane 2 is proportional to the Fourier transform of the amplitude $U_1(\xi,\eta)$. In practice we can ignore the constant of proportionality and simply write

$$U_2(x,y) = \tilde{U}_1(x/\lambda f, y/\lambda f) \quad , \tag{4.1}$$

where the tilde denotes the Fourier transform. Eq.(4.1) ignores the fact that the diameter of the lens is finite: its effect is not difficult to incorporate but we shall ignore it as it complicates the essential simplicity of the analysis.

The second optical system also performs a Fourier transform between planes (2) and (3):

$$U_3(\xi',\eta') = \tilde{U}_2(\xi'/\lambda f, \eta'/\lambda f) \tag{4.2}$$

and combining Eqs.(4.1) and (4.2) we see that the complex amplitude in plane (3) is a unit magnification inverted image of that in plane (1):

$$U_3(\xi',\eta') = U_1(-\xi,-\eta) \quad . \tag{4.3}$$

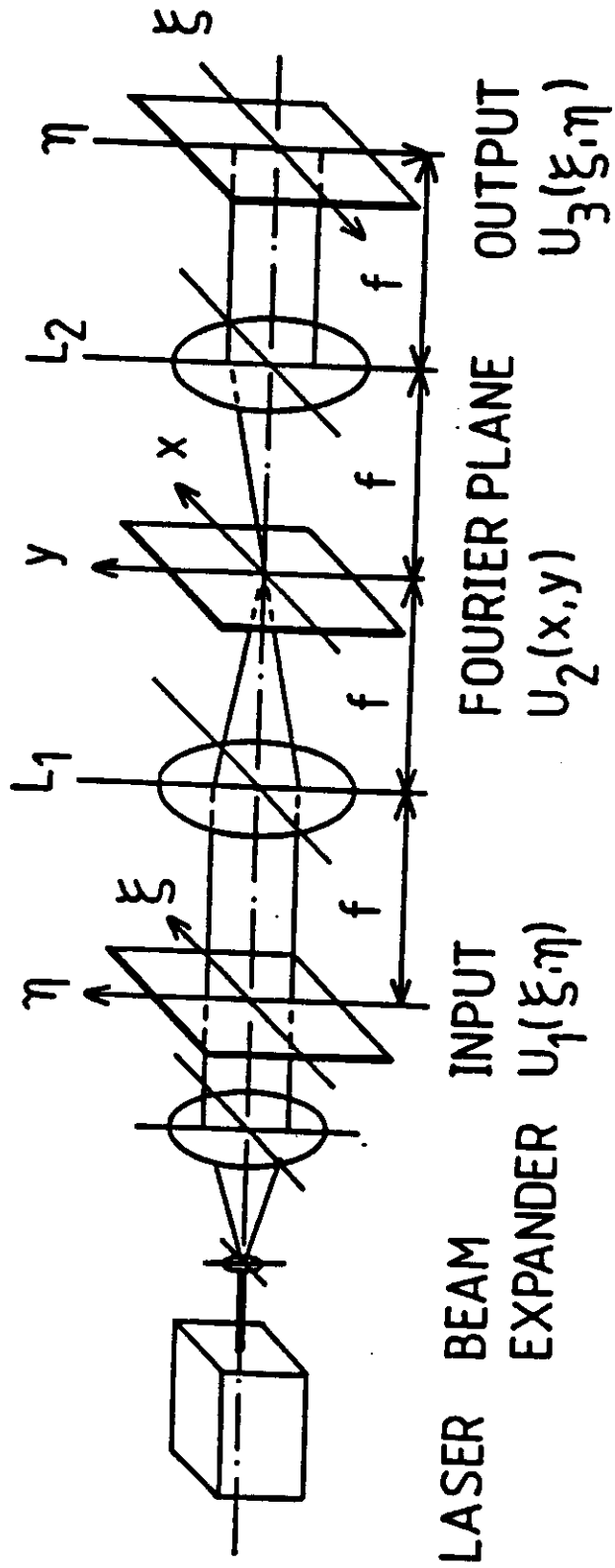

Figure 4.1 The coherent optical processor. The complex amplitude $U_2(x,y)$ is the Fourier transform of the amplitude $U_1(\xi,\eta)$: the complex amplitude $U_3(\xi',\eta')$ is the Fourier transform of $U_2(x,y)$ and thus $U_3(\xi',\eta') = U_1(-\xi,-\eta)$, excluding aperture effects.

This result is obvious from geometrical optics. The power of the coherent optical processor is that we have access to the Fourier transform of the input and by altering the complex amplitude in this plane (i.e. 'spatial filtering') we can alter the appearance of the image. Simple spatial filtering is discussed in the following section.

4.2 Simple Spatial Filtering

The complex amplitude $U_2(x,y)$ in the back focal plane of the first Fourier transform lens in Fig 4.1 is of course a complex function (has a modulus and a phase) and in general optical spatial filtering involves modifying this using a complex spatial filter (i.e. one which alters both the modulus and phase of U_2). Methods of accomplishing this are discussed in Section 5. However, the basic principles of optical spatial filtering, as first demonstrated in 1893 by Abbe, can be illustrated using modulus-only filters (i.e. simple absorption filters) such as slits and circular apertures. Figure 4.2(b) shows an object consisting of a mesh and the intensity of its Fourier transform as it appears in plane (2) is shown in 4.2(a). The Fourier transform is a map of the spatial frequency content of the object and in this case we see from Fig 4.2(a) that the object consists of a number of discrete frequencies (terms in a Fourier series) spread over the (u,v) spatial frequency plane. If a horizontal slit is placed in the Fourier plane (2), as in Fig 4.2(c), then only the zero frequency (DC term) is transmitted in the vertical direction and the resulting image (Fig 4.2(d)) contains no detail in the vertical direction - we have 'filtered out' the vertical spatial frequencies, leaving structure only along the horizontal axis. Similarly, Figs 4.2(e) and (f) show the effect of a vertical slit in the Fourier plane.

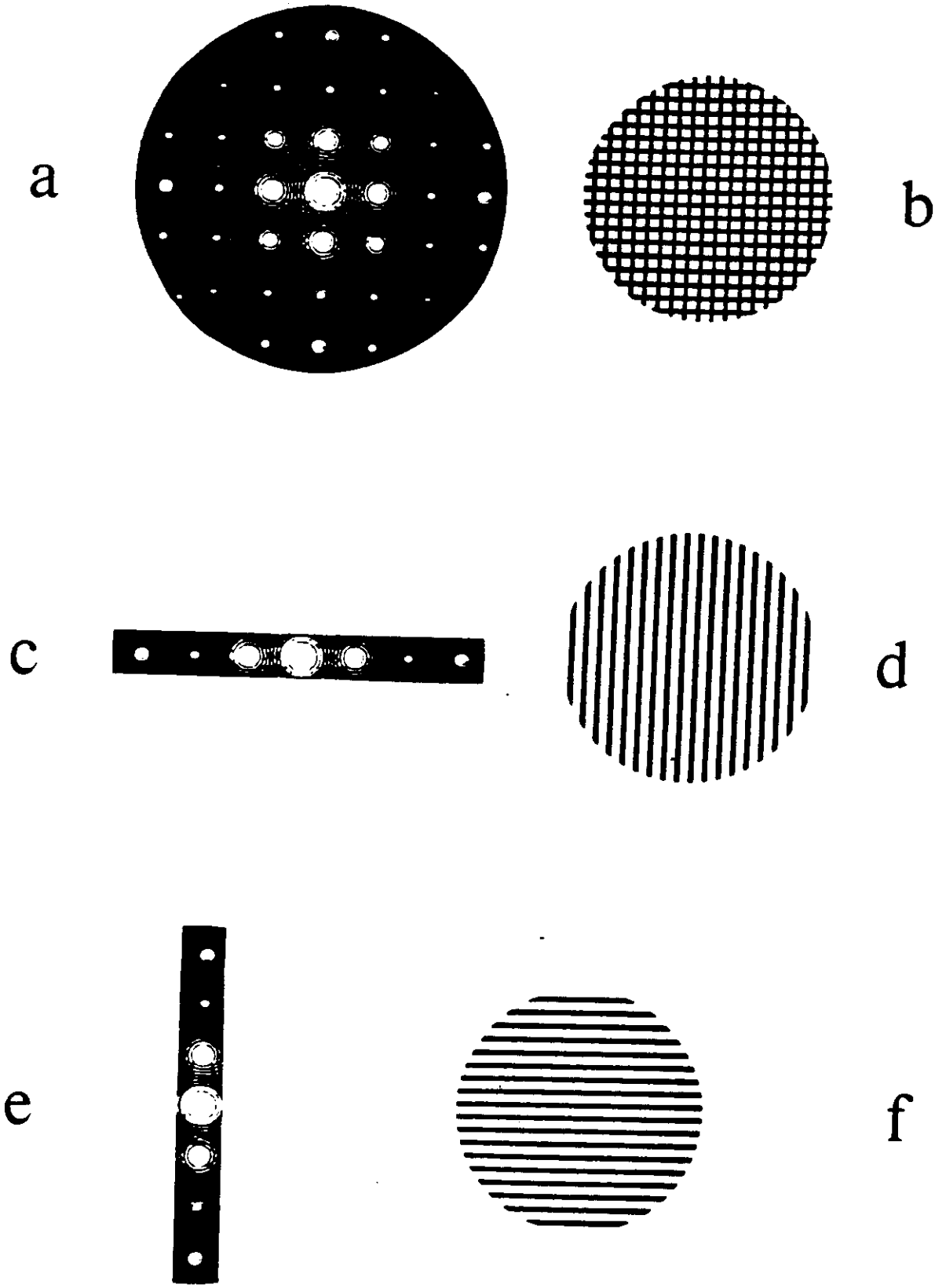

Figure 4.2 Optical spatial filtering. (a) unmodified spectrum (b) object (c) spectrum modified by horizontal slit (d) resultant image (e) spectrum modified by vertical slit (f) resultant image. (From Goodman, see Introduction).

5. COMPLEX SPATIAL FILTERING

5.1 Phase-Contrast Microscopy

Probably the first application of complex spatial filtering was to the visualisation of the phase of an object wave by phase-contrast microscopy. The complex amplitude for an input phase object can be written

$$U_1(\xi,\eta) = \exp(i\phi(\xi,\eta)) \quad , \tag{5.1}$$

where $\phi(\xi,\eta)$ is the phase. If the phase is small, $\phi \ll 1$, we can write,

$$U_1(\xi,\eta) = 1 + i\phi(\xi,\eta) \quad , \tag{5.2}$$

so that without any spatial filtering the image intensity is simply constant:

$$\begin{aligned} I_3(\xi',\eta') &= |U_1(-\xi,-\eta)|^2 \\ &= 1 \end{aligned} \tag{5.3}$$

However, by inserting a spatial filter in the Fourier plane (2) we can produce an image intensity variation proportional to the phase of the object. The complex amplitude in the Fourier plane is

$$U_2(x,y) = \delta(x,y) + i\tilde{\phi}(x,y) \tag{5.4}$$

Now we insert a small phase disc, of phase retardation $\pi/2$ ($\exp[i\pi/2] = i$) at the centre of the Fourier plane so that the complex amplitude is now

$$U_2(x,y) = i[\delta(x,y) + \tilde{\phi}(x,y)] \tag{5.5}$$

and the image intensity is

$$I_3(\xi',\eta') \sim 1 + 2\phi(-\xi,-\eta) \qquad (5.6)$$

Thus, for weak phase objects, the image intensity is proportional to the phase of the object wave. The phase-contrast microscope works on this principle and is an elementary example of complex spatial filtering. The spatial filter is not difficult to construct in this case.

5.2 Van der Lugt Filters

Consider the possible application of a coherent optical processor to image deblurring or sharpening. A normal incoherent optical image $i(\xi,\eta)$ is equal to the object intensity $o(\xi,\eta)$ convolved with the point spread function $p(\xi,\eta)$ of the imaging system,

$$i(\xi,\eta) = o(\xi,\eta) * p(\xi,\eta) \; . \qquad (5.7)$$

In order to recover the original object intensity from the image intensity we have to multiply the spectrum of $i(\xi,\eta)$ by a suitable filter function $H(u,v)$. In the absence of any noise (this is obviously an idealisation), the optimum filter is simply the inverse filter,

$$H(u,v) = 1/P(u,v) \qquad (5.8)$$

since it is clear from the Fourier transform of Eq.(5.7) that

$$O(u,v) = I(u,v)\;[1/P(u,v)] \; . \qquad (5.9)$$

In general, when there is noise present, the inverse filter (5.8) is not the best choice, but nevertheless the filter $H(u,v)$ is usually

complex, as in Eq.(5.8). In optical terms, the filter transmission must have a phase and a modulus (absorption) component.

The van der Lugt filter (IEEE Trans Information Theory, IT-10, 139 (1964)) is a way of making a complex filter using an absorption-only medium such as a photogaphic emulsion. It is essentially a Fourier-hologram. One arrangement for making a van der Lugt or holographic filter is shown in Fig 5.1. If we wish to make a filter H(u,v) we start with an object whose amplitude transmittance is $h(\xi,\eta)$. The complex amplitude at the focal plane of L_1 in Fig 5.1 is therefore H(x,y). Before recording, we coherently add this to a plane wave reference beam at angle θ whose complex amplitude is

$$U_r = \exp(-2\pi i\alpha y) \quad ,$$

where the spatial frequency $\alpha = \sin\theta/\lambda$. This frequency is chosen to be greater than the highest frequency present in H(u,v) by ensuring that the angle θ is greater than three times the convergence semi-angle of light from lens L_1.

The intensity in the hologram plane is therefore given by

$$I(x,y) = | H(x,y) + \exp(-2\pi i\alpha y) |^2 \quad . \qquad (5.10)$$

As in ordinary holography, there are four terms in the expansion: the term $H(x,y).\exp[2\pi i\alpha y]$ is of most importance. If the holographic recording medium has a linear relationship between incident intensity and amplitude transmittance after development, the complex amplitude transmittance will also have the four terms, with the term involving $H(x,y).\exp[-2\pi i\alpha y]$ again being the important term.

Note that we required a complex filter H(x,y) but have in fact made one with complex transmittance proportional to $H(x,y).\exp[2\pi i\alpha y]$. If we insert this filter into the Fourier plane (2) of the coherent optical processor of Fig 4.1, then the 'corrected' (e.g. deblurred) image will appear at plane (3), but centred at $\eta' = -\alpha\lambda f$ instead of at the origin:

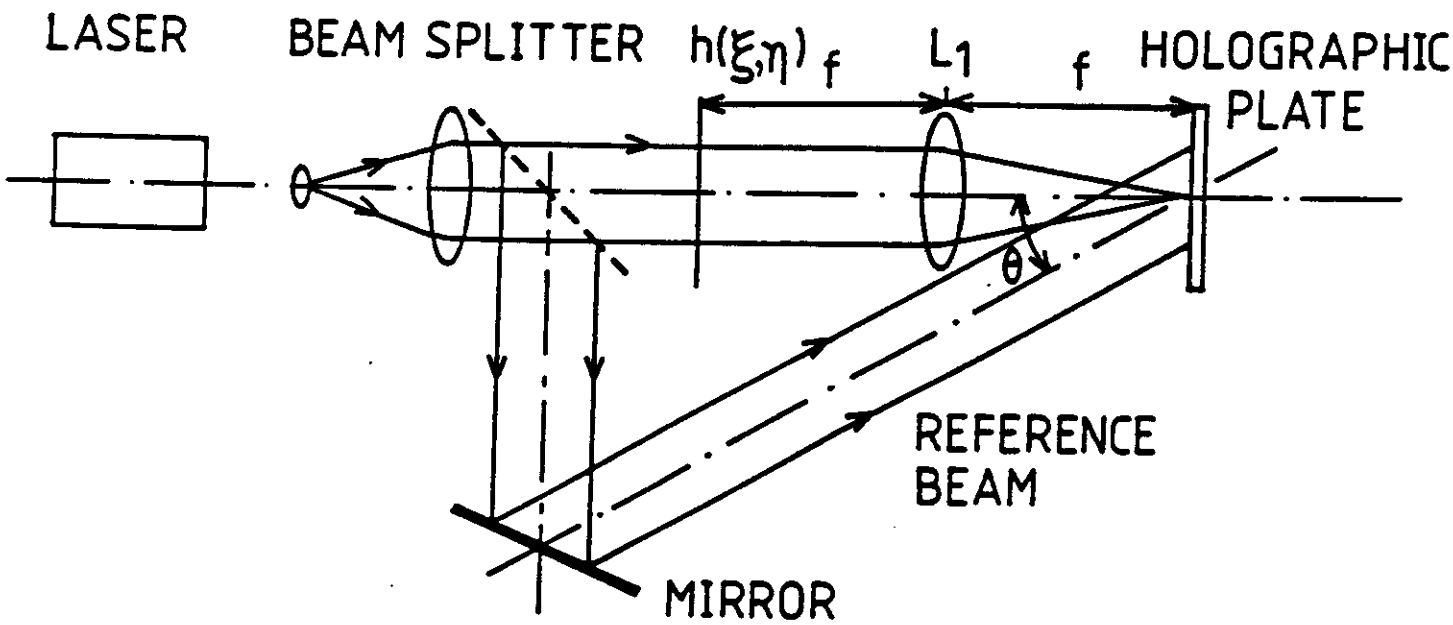

Figure 5.1 Interferometric arrangement for recording a van der Lugt or holographic filter

this is because multiplication by exp[2πiαy] in plane (2) is equivalent to convolution by $\delta(\eta' + \alpha\lambda f)$ in plane (3). The other terms in the expansion of (5.10) give spurious (unwanted) images centred at the origin and at $\eta' = \alpha\lambda f$, but these images do not overlap the important one centred at $\eta' = -\alpha\lambda f$, provided that α is large enough.

Although the van der Lugt or holographic filter has been described for inverse filtering, its most practical application is to so-called 'matched filtering' for the automatic recognition of patterns, characters, etc and this is described in Section 6.

5.3 Computer-generated holograms

A major drawback of van der Lugt filters is that the inverse Fourier transform $h(\xi,\eta)$ of the filter function $H(u,v)$ is required in order to make the filter. For inverse filters in particular it is almost impossible to realise $h(\xi,\eta)$, which is the function that deconvolves the point spread function of the imaging system (it is easier to make the filters required for matched filtering, see Section 6).

The technique of making holograms using a computer output device was pioneered by Lohmann (see Appl Optics 7, 651-655 (1968) and references therein). Because of the binary nature of many computer-output devices, computer-generated holograms usually have only clear and opaque areas. In phase detour CGHs the modulus and phase characteristics of the hologram are formed in the following way, see Fig 5.2(a) and (b). Each sampling point (n,m) in the hologram is represented by a square of side d. A clear aperture within the square is adjusted in area to give the required amplitude transmission for that pixel - this provides the correct modulus of the hologram element. The displacement δ of the clear aperture from the centre of the pixel gives an additional path length $\lambda\delta/d$ and thus phase associated with that pixel.

If the wavefront to be recorded (and reconstructed) contains only phase variations, then the fringe positions can simply be encoded in a binary computer generated interferogram. The fringe maxima and minima are encoded as transmitting and opaque bands. Fig. 5.3 shows a result of this technique which is particularly important for wavefront testing.

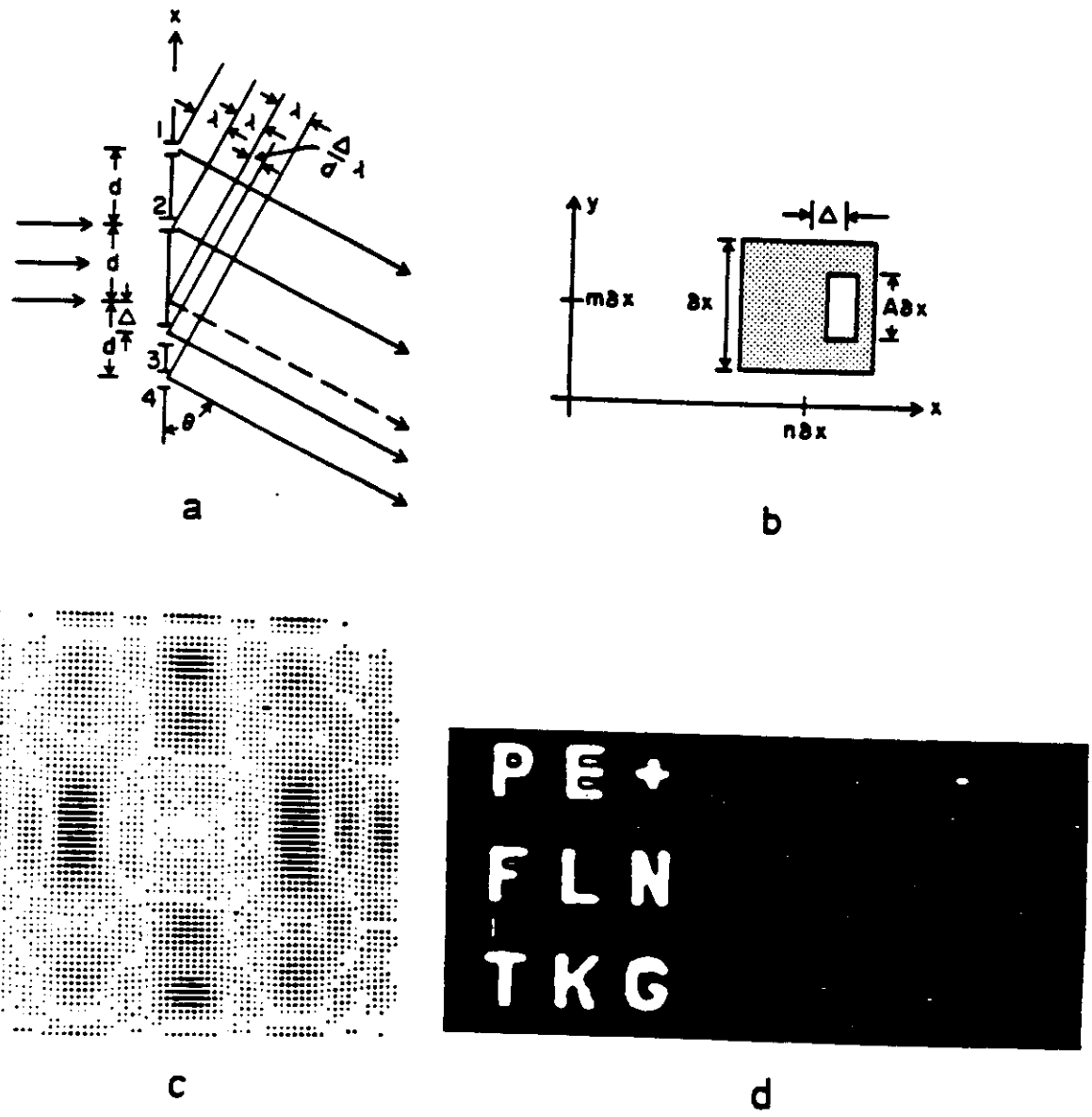

Figure 5.2 (a), (b) Operation of a binary computer-generated hologram: (c) example of hologram (d) reconstruction of (c) (after Lohmann)

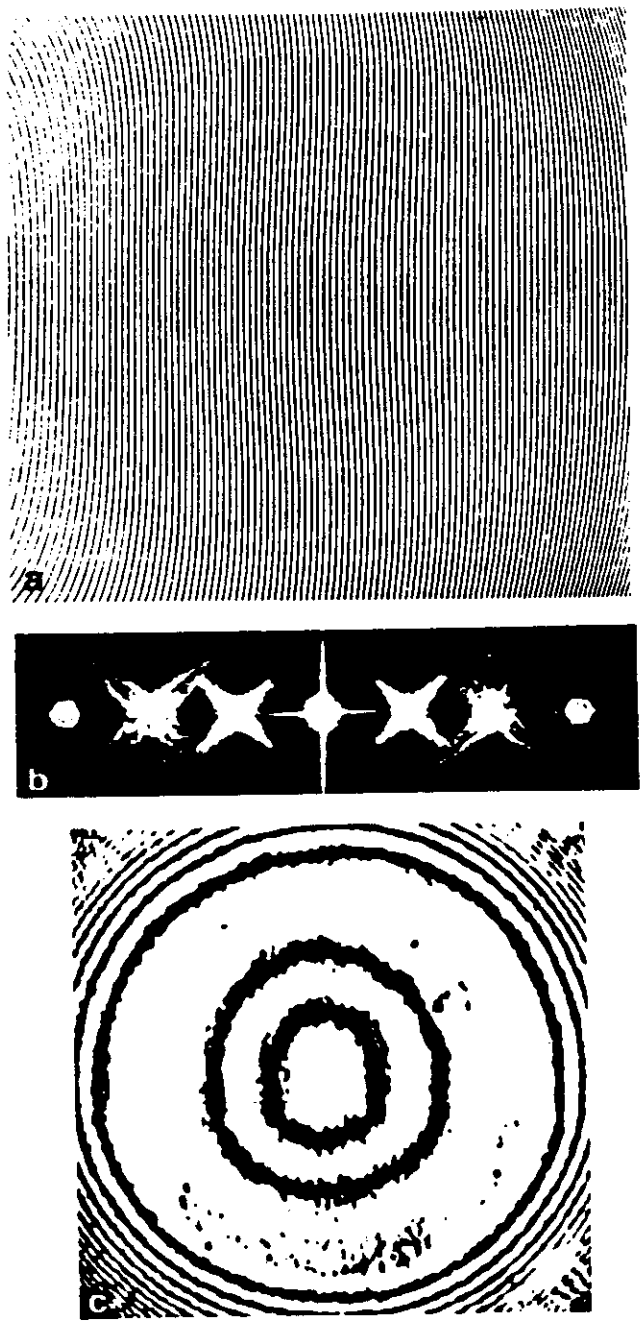

Figure 5.3 (a) Computer-generated hologram of an aspheric wavefront
(b) The Fraunhofer diffraction pattern of (a)
(c) The interference pattern of the reconstructed wave from the hologram with a plane reference wave.

6. MATCHED FILTERING AND PATTERN RECOGNITION

6.1 The Matched Filter

When discussing van der Lugt filters in Section 5.2, we considered the case of making an inverse filter H(u,v). This filter has the property that, when inserted in the Fourier plane (2) of a coherent optical processor, it produces a deblurred or sharp image from a blurred or degraded input, centred off-axis at $\eta' = a\lambda f$. In this case, both input and output are similar, the output simply being an improved version of the input.

Other filters can be constructed for other tasks. For example, suppose that we wish to identify each occurrence of a certain character in a page of characters. In this case, our output need only be a bright point at the location of each occurrence. It can be shown that, when additive gaussian 'white' noise is present, the optimum filter in this case is the matched filter.

Let $s(\xi,\eta)$ be the particular signal of interest (e.g. the letter 'e'). The matched filter has a point spread function $h(\xi,\eta) = s^*(-\xi,-\eta)$ and a Fourier transform $H(u,v) = S^*(u,v)$, where S(u,v) is the Fourier transform of the signal of interest.

6.2 Optical Implementation

An optical matched filter is easily constructed by the van der Lugt method (see Fig 5.1). For a real signal (the usual case), the input is simply an upside-down version of the signal of interest. The intensity in the hologram recording plane is, c.f. Eq.(5.10),

$$I(x,y) = | S^*(x,y) + \exp(-2\pi i a y) |^2 \qquad (6.1)$$

where S(x,y) is the optical Fourier transform of the signal $s(\xi,\eta)$. Assuming linearity of the holographic recording medium, the amplitude transmittance of the hologram, t(x,y) has four components:

$$t(x,y) = 1 + |S|^2 + S^* \exp(-2\pi i\alpha y) + S \exp(+2\pi i\alpha y). \quad (6.2)$$

Suppose that this matched filter is placed in the Fourier plane (2) of a coherent optical processor (see Fig 4.1) and that an arbitrary signal $g(\xi,\eta)$ is placed in the input plane (1). The signal $g(\xi,\eta)$ may or may not contain the signal of interest. Immediately after the Fourier plane we now have $G(x,y).t(x,y)$. Substituting for $t(x,y)$ from Eq.(6.2), there are four terms:

$$\begin{aligned} &\text{(i)} && G(x,y) \\ &\text{(ii)} && G(x,y)\ |S(x,y)|^2 \\ &\text{(iii)} && G(x,y)\ S^*(x,y)\ \exp(-2\pi i\alpha y) \\ &\text{(iv)} && G(x,y)\ S(x,y)\ \exp(+2\pi i\alpha y) \end{aligned} \quad (6.3)$$

The first two terms give an output in plane (3) that is centred at the origin. The third term gives the <u>cross-correlation</u> of $g(\xi,\eta)$ and $s(\xi,\eta)$ and the fourth gives the <u>convolution</u> of $g(\xi,\eta)$ and $s(\xi,\eta)$. The third is the important one in matched filtering. Suppose that the unknown signal <u>is</u> in fact the signal of interest - in that case, $G(x,y) = S^*(x,y)$ so that all phase effects, except the plane wave, in term (iii) of Eq.(6.3) are zero. This means that the second Fourier transform lens will focus the light to a bright spot in the final output plane.

6.3 <u>Examples</u>

Fig 6.1 shows an optical correlator for matched filtering. Fig 6.2 shows an example of character recognition (upper) and the detection of a signal in noise (lower). Figure 6.3 shows the full cross correlation matrix for 25 diatoms. Each diatom is cross-correlated with all others and the strong component along the diagonal shows that each diatom can be identified correctly using this technique.

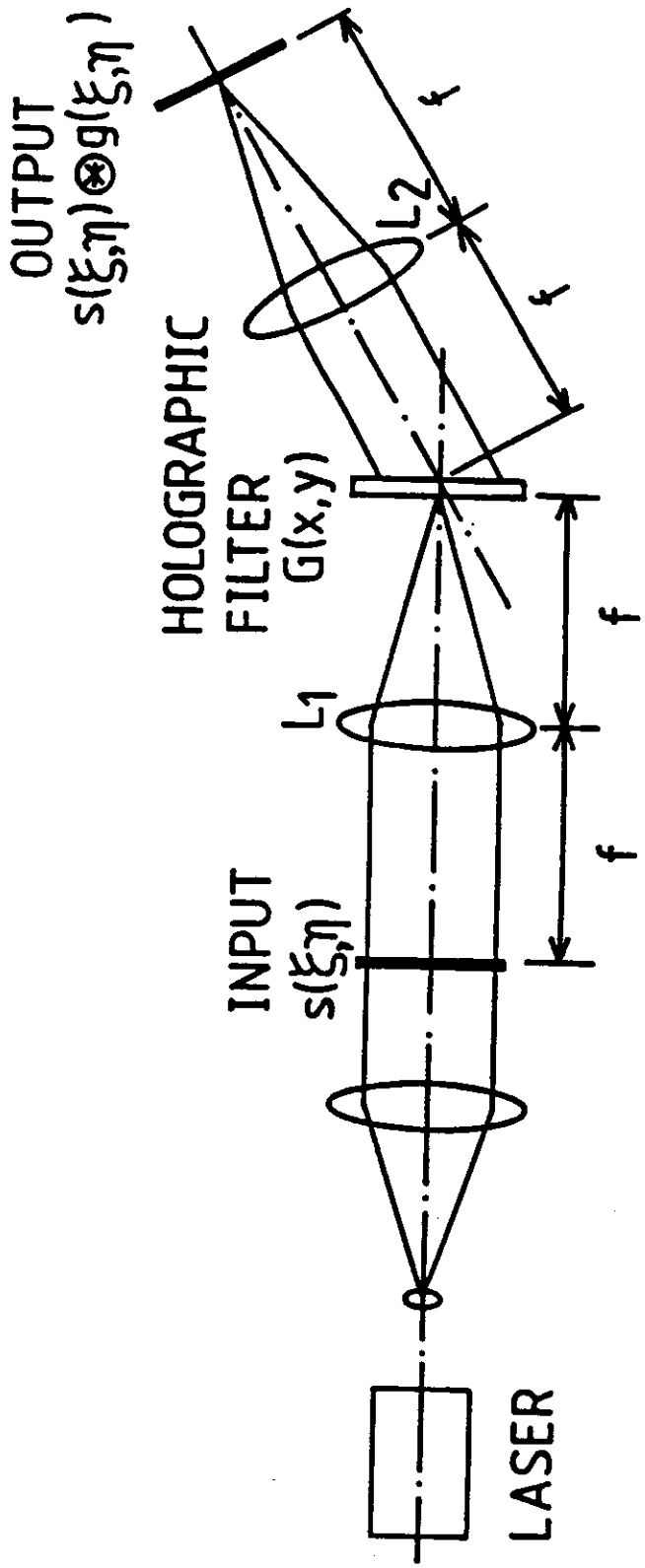

Figure 6.1 Optical correlator using a holographic filter

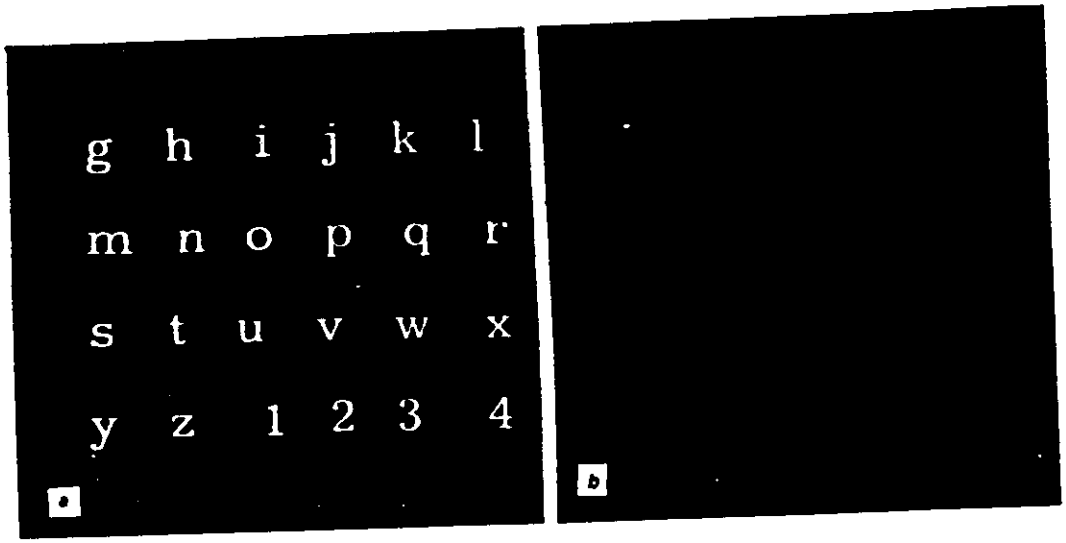

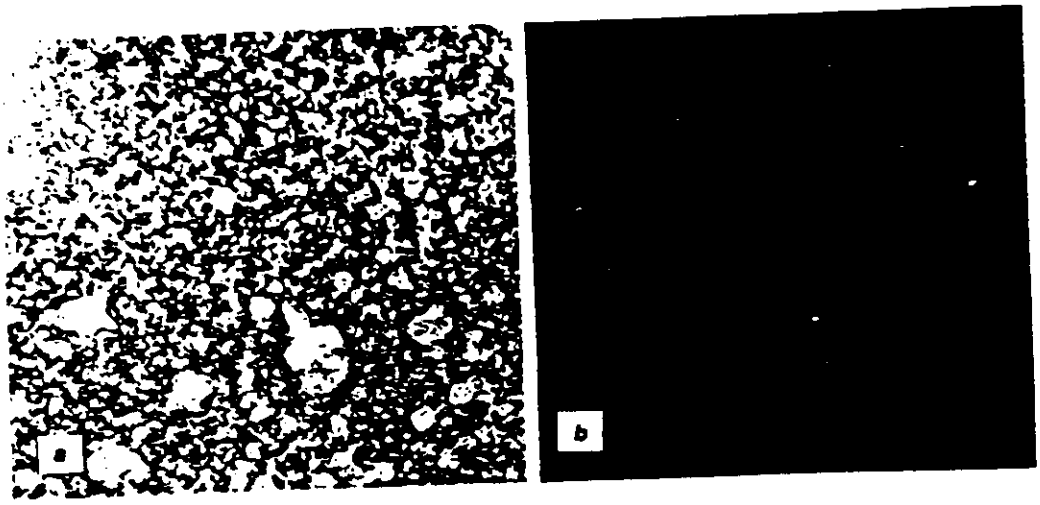

Figure 6.2 Examples of the use of optical matched filtering in character recognition and signal detection. (From F T S Yu, see Introduction: original by van der Lugt)

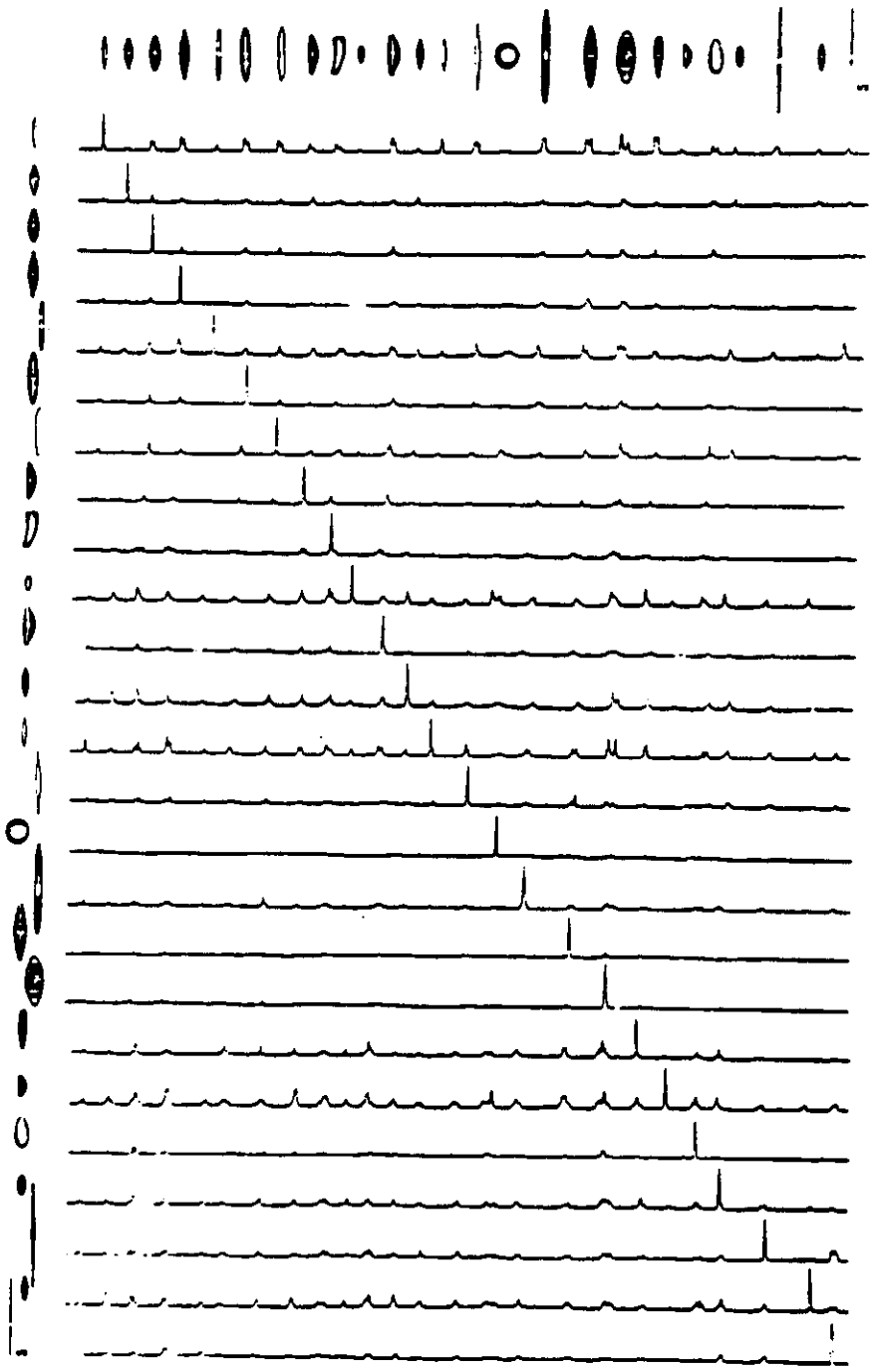

Figure 6.3 A 25 x 25 correlation matrix obtained with spatial filters of each diatom compared against all 25 diatoms. (By S P Almeida)

6.4 Matched Filtering by Degenerate Four Wave Mixing

Matched filtering is achieved by multiplying the Fourier transform of the unknown signal by the complex conjugate of that of interest, i.e. $G(u,v)\ S^*(u,v)$. The transform of this product is a cross-correlation of $g(\xi,\eta)$ and $s(\xi,\eta)$ and shows large peaks at points where the unknown $g(\xi,\eta)$ matches the signal of interest $s(\xi,\eta)$. When $S^*(u,v)$ is in the form of a transparency, as with the van der Lugt filter, then the multiplication is carried out simply by illuminating the transparency by $G(u,v)$.

Suppose, however, that $S^*(u,v)$ is <u>not</u> available in the form of a transparency, i.e. for one reason or another it is not possible to make a matched filter. (Perhaps the signal $s(\xi,\eta)$ is only available in transparency form.) In this case the product can be performed by degenerate four wave mixing (DFWM) in a non-linear crystal such as bismuth silicon oxide (BSO), as first shown by Pepper et al (Opt Lett 3, 7-9 (1978)).

The method is illustrated in Fig 6.4. DFWM is a generalised form of real-time holography. In Fig 6.4(a), imagine that beam 1 is a reference beam and beam 3 is an object beam - together they form a hologram. If this hologram is illuminated by beam 2, one reconstructs the object beam of travelling in the opposite direction to the original object beam 3. In fact, beam 4 is the phase conjugate of beam 3 if beams 1 and 2 are plane waves. If <u>all three</u> beams 1,2 and 3 illuminate a suitable non-linear crystal <u>simultaneously</u>, then under the appropriate conditions one obtains a fourth beam whose complex amplitude is proportional to the <u>product</u> of beams 1, 2 and 3. This can form the basis of an optical correlator for matched filtering and other applications.

Referring to Fig 6.4(b), let the complex amplitude incident on the BSO crystal due to beam 2 be a plane wave u_2 and let the complex amplitudes after planes 1 and 3 (which contain the fields to be correlated) be u_1 and u_3. The lenses L_1 and L_3 perform the Fourier transform, U_1 and U_3 on these fields, so that a total of three fields u_2, U_1 and U_3 are incident on the crystal. They induce a non-linear polarisation

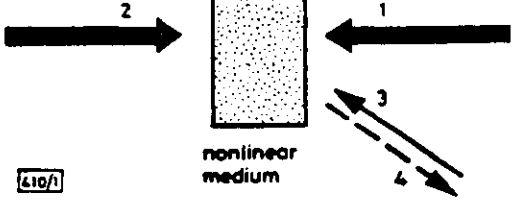

a

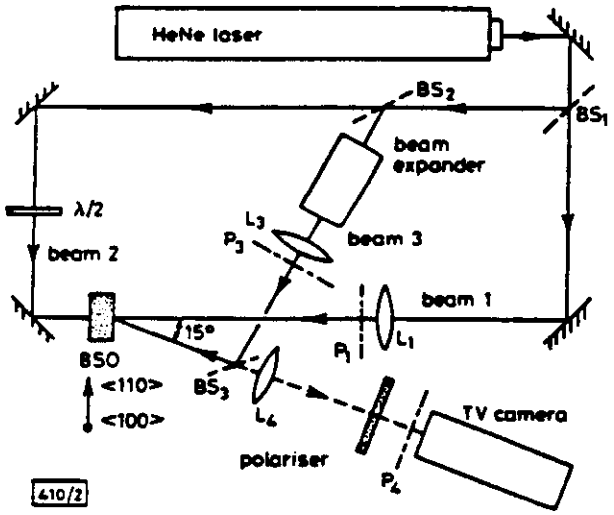

b

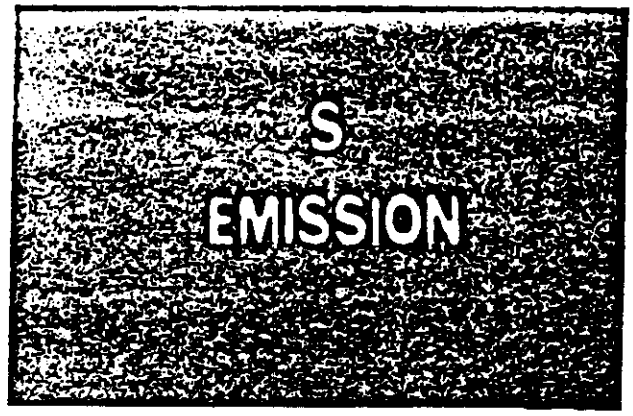

a

c

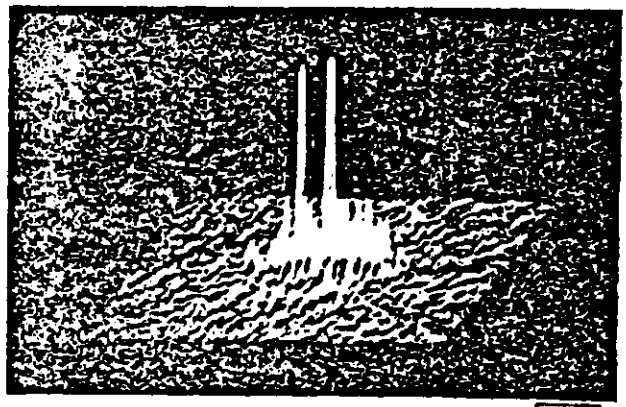

b

410/3

Figure 6.4 (a) Basic configuration for DFWM
(b) Schematic diagram of image correlator
(c) Upper: inputs to correlator
Lower: correlator output showing correlation peaks
(From Petts et al, Electronics Lett, 20, 32-33 (1984))

$$P = X^{(3)} U_1 u_2 U_3^* ,$$

where $X^{(3)}$ is the third-order non-linear susceptibility of the medium. This induced polarisation produces a fourth (output) field U_4 and since u_2 is a plane wave,

$$U_4 \propto U_1 U_3^* .$$

This is the product of Fourier transforms required for matched filtering and the lens L_4 performs the final Fourier transform necessary to display the correlation peaks.

The advantage of DFWM is that there is no need to make a matched filter provided the input for the signal-of-interest is available in transparency form. As with many coherent optical processors, the inputs may be provided through various electro-optic devices (see Section 8). Fig 6.4(c) shows an example of character recognition using this technique. For a review of information processing using DFWM, see White and Yariv, Opt Engng, 21, 224-230 (1982).

7. SYNTHETIC APERTURE RADAR (SAR)

One of the most successful applications of coherent optical information processing has been in the formation of high-resolution maps from synthetic aperture radar data. This technique was developed by Cutrona et al (Proc IEEE, 54, 1026-1032 (1966)). In this section we give only a brief outline of the method, stressing the basic principles. For a review, see K Tomiyasu (Proc IEEE 66, 563-584 (1978)) or E N Leith in the book edited by Casasent (see Introduction).

Figure 7.1(a) illustrates the terminology. A side-looking radar on an aircraft has an intensity pattern on the ground called the 'beam foot-print'. Th aircraft flies along the azimuth direction, the direction perpendicular to azimuth along the ground being called the range. The beam 'look-angle' is θ and the range along θ is called the slant-range.

The name 'synthetic aperture' is derived from the method of (coherent) imaging in azimuth, shown in Fig 7.1(b). Here and below we consider the imaging of a point scatterer - the image of an extended object can clearly be constructed from many point images. The radar emits pulses at t_1, t_2,.....t_n, and the time taken for the pulse to return to the aircraft clearly depends on r_1, r_2,....r_n. Figures 7.2(a) and (b) show that the time delay varies parabolically with the flight time as the aircraft makes its closest approach to the point object. If the return signal is heterodyned ('interfered') with a local oscillator on board the aircraft, the signal shown in the lower part of Fig 7.2(b) is obtained. This signal, when recorded on film is simply a (one-dimensional) hologram of a point source and can be reconstructed in the normal optical way, see Fig 7.2(c). Note that the angular resolution depends on the extent of the azimuth flight - this may be 1km, giving an angular resolution of 10^{-4} rad (e.g. 1m at 10km) for λ = .1m radar.

Imagery in range is simply achieved by timing the delay between transmission and reception of the pulse and the use of a frequency-modulated pulse gives the highest resolution for the lowest power, see Fig 7.3(a). The FM or 'chirp' pulse is also a hologram of a

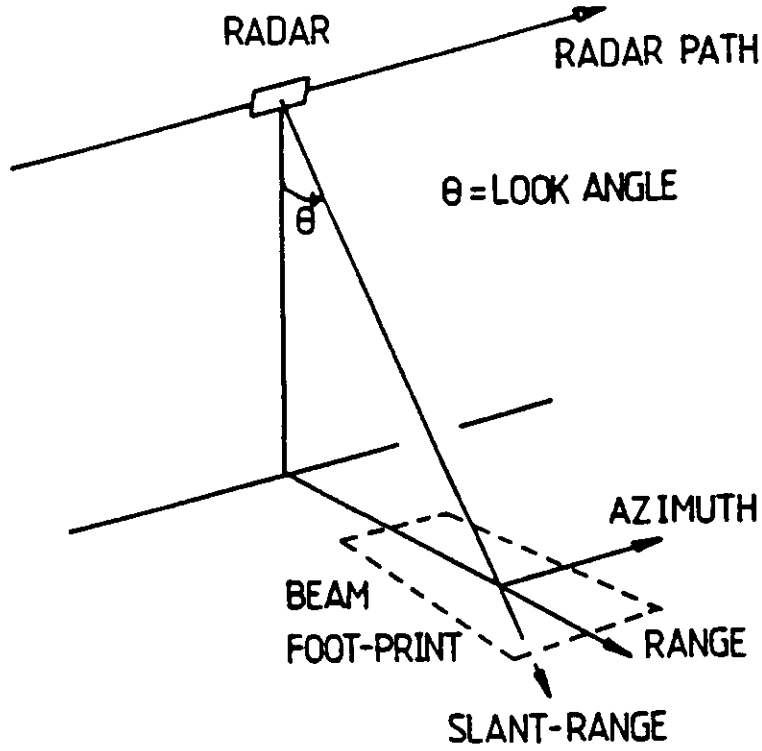

SYNTHETIC APERTURE IN AZIMUTH

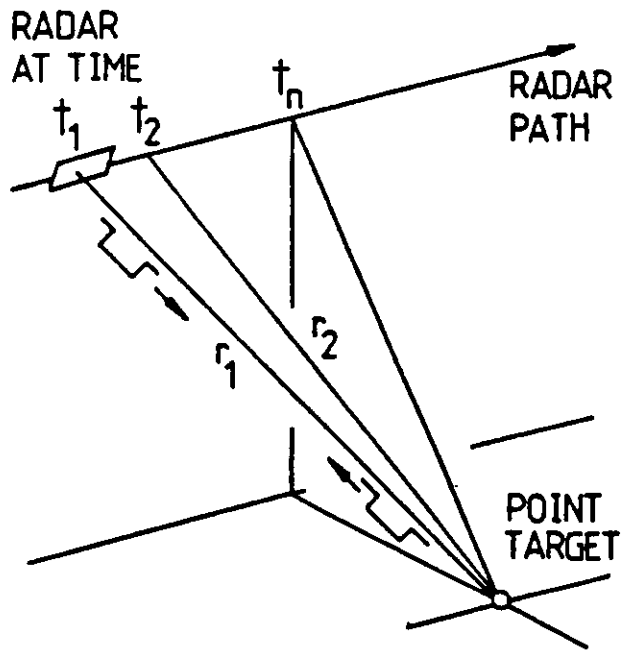

Figure 7.1 (a) Terminology of synthetic aperture radar
(b) Imaging by the synthetic aperture in azimuth
(Courtesy of K Ouchi)

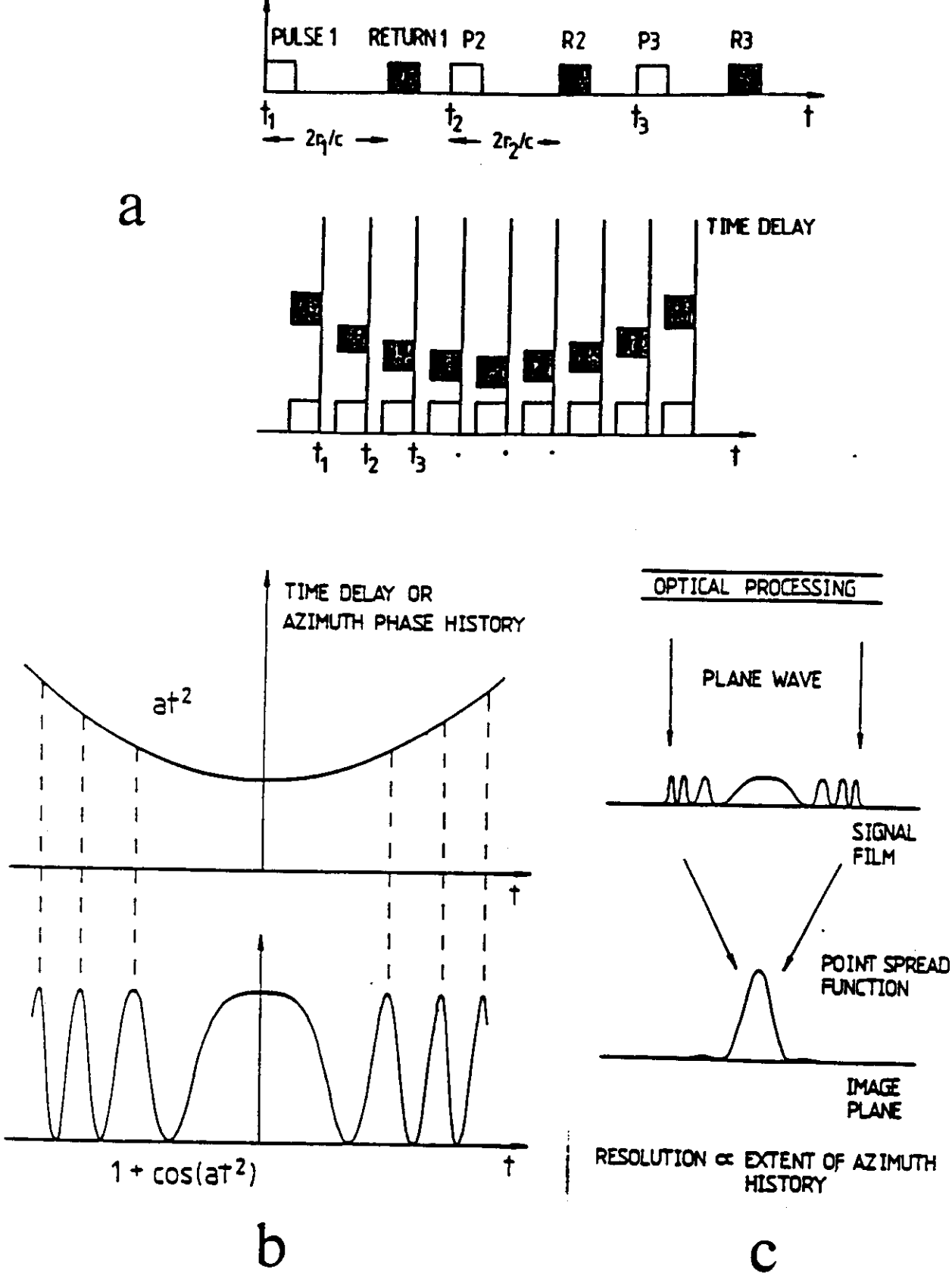

Figure 7.2 (a) Pulse-return time delay as a function of flight time to around closest approach to a point object
(b) Interference with a local oscillator to produce a hologram in the azimuth direction.
(c) Optical reconstruction of the hologram
(Courtesy of K Ouchi)

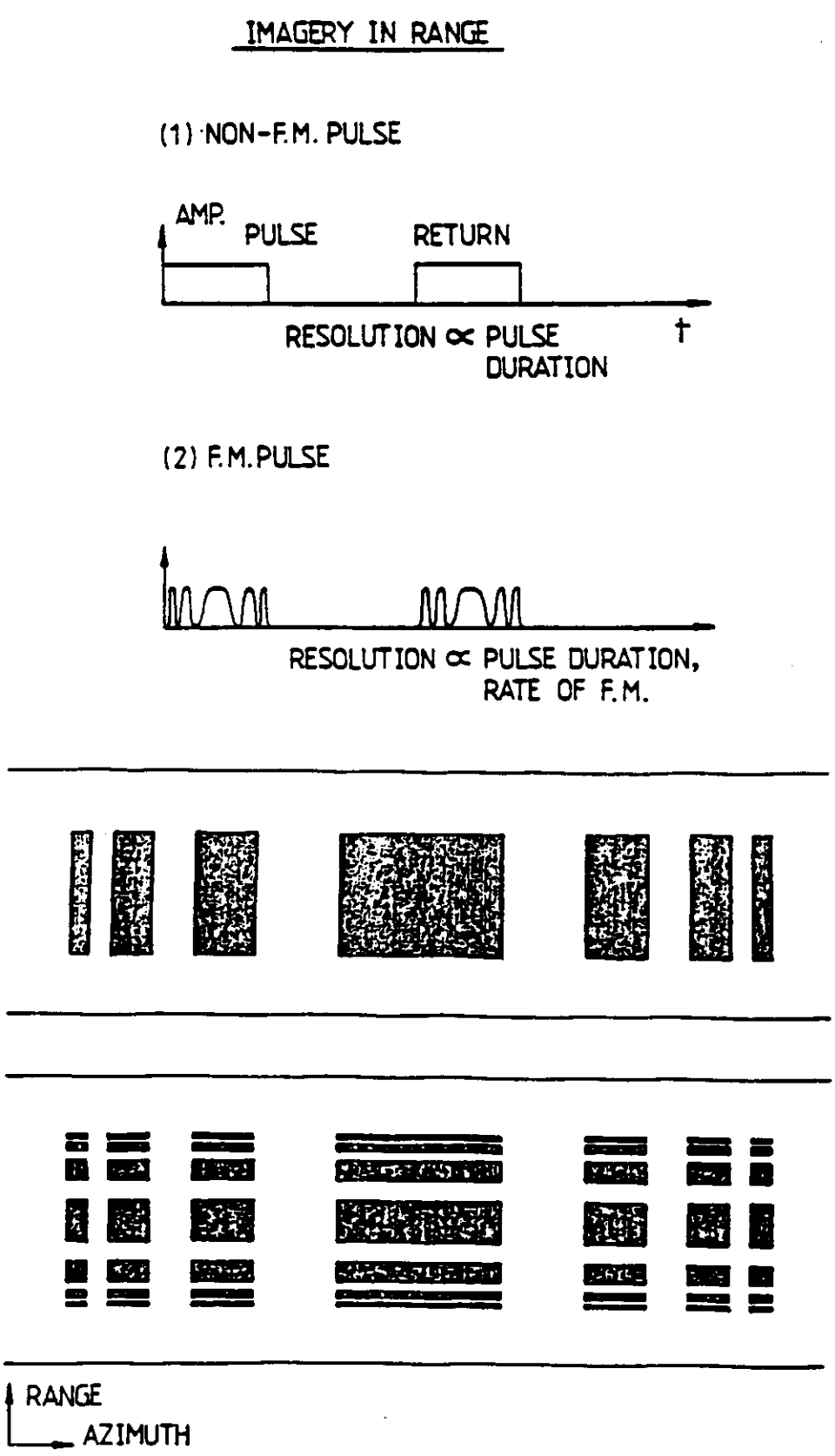

Figure 7.3 (a) Imagery in range
(b) Film recording in range and azimuth for a point object
(Courtesy of K Ouchi)

point object, so that the final two-dimensional film recording is a hologram in both the range and azimuth directions, as shown in Fig 7.3(b).

This hologram can be reconstructed by the simple coherent optical system shown in Fig 7.4. The 'focal lengths' of the hologram are different along the range and azimuth directions and these can be compensated by using two cylindrical lenses in the optical system.

The above processor is somewhat oversimplified, since the focal length of the azimuth hologram clearly depends on the range of the point scatterer (see Fig 7.2). This can be compensated by using a conical lens placed in contact with the hologram. An improved tilted plane processor is described in Kozma et al, Appl Opt 11, 1766-1777 (1972).

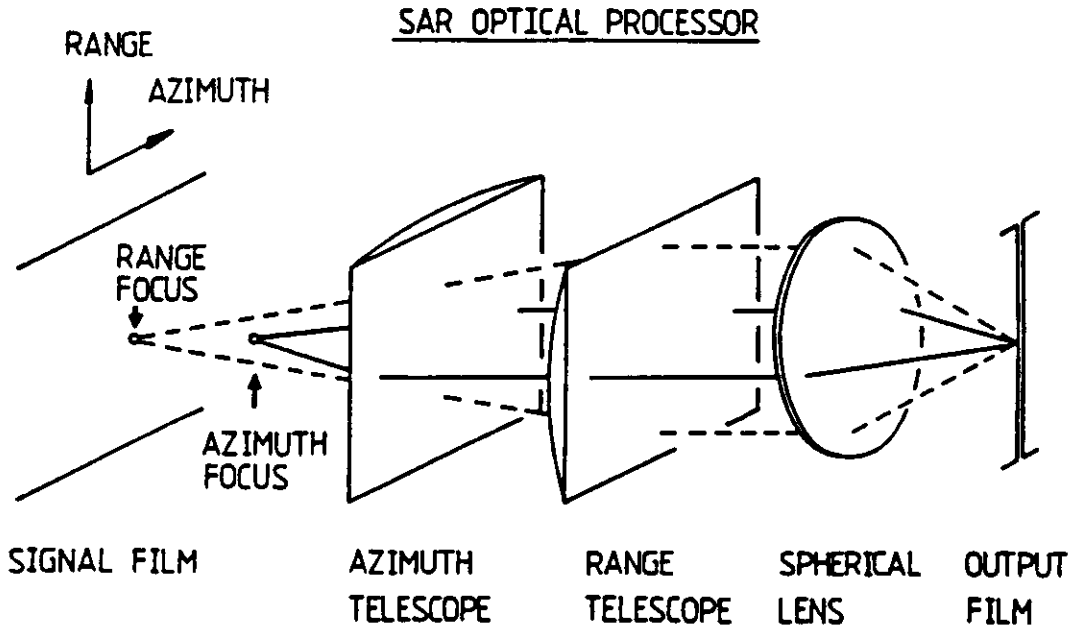

Figure 7.4 SAR Optical Processor (Courtesy of K Ouchi)

8. REAL-TIME INPUT DEVICES

The nature of coherent optical processing requires that the signal being analysed be transformed to a suitable input medium - in previous Sections we have assumed that this is photographic film. Although photographic materials have many advantages, particularly high speed and large storage capacity, they require chemical development to render the recorded image visible and are not suitable as real-time input devices to a coherent optical processor.

A typical application for a real-time device, or spatial light modulator, would be in a character-recognition system. A page of printed characters are illuminated with spatially incoherent light (to avoid the problems of speckle). The image has to be converted so as to modulate the complex amplitude of a coherent light beam. (The second input in this case would probably be a set of van der Lugt filters of individual characters pre-recorded on film.) The real-time device that transforms the signal is sometimes called an 'incoherent-to-coherent convertor'. In other applications, we may wish to use an electronic signal to modulate the complex amplitude of a coherent light beam.

A recent review of spatial light modulators for coherent optical processors has been given by G R Knight (in the book edited by Lee, see Introduction). Figure 8.1 summarises the main characteristics of a number of devices. Compared to photographic film, which has a writing energy of approximately 10^{-2} ergs/cm^2, all of the devices are fairly insensitive and the time-response of several devices is on the order of milliseconds.

As an example, we shall briefly describe the liquid crystal light valve (LCLV) which is a commercially available device. Its construction is shown in Fig 8.2. The light blocking layer and dielectric mirror serve to isolate the writing beam of light from the reading beam, which operates in reflected light. The insulating layers are overcoated with sputtered SiO_2 films that are ion-beam etched at an angle to provide twisted nematic alignment for the liquid crystals. In the reading process, light travels twice through the liquid crystal layer, which is typically 2μm thick.

	Decay time	Uniformity	Life	Coherent image	Comp. erase	Size	Oper. temp.
1. Liquid crystal light valve	15 ms	$<2\lambda$		Yes	Yes	2.5 × 2.5 cm	Room
2. e-Beam KDP (Titus tube)	Semi-permanent erase < 1 ms with flood e-beam	Needs improvement		Yes	Yes (at −52 °C)	5.1 × 5.1 cm	−52 °C
3. PROM	Several hours: erase < 6 ns optical flood	$<\lambda/6$	Long	Yes	Yes	4 cm diameter	Room
4. Photo-Titus (KDP):	> 1 h erase < 10 ns flood light	$<\lambda/2$		Yes	Yes	4 cm diameter	−50 °C
$(Bi_4Ti_3O_{12})$				Yes	Yes	1 cm × 1 cm	
5. Ceramic ferroelectrics (strain biased)	10–50 μs switching	(Poor) local strain variations	Long ($> 10^9$ cycles	Yes	Yes	> 3.25 cm diameter	Room
(scattering)	10–50 μs switching		Long	No	Yes	> 3.25 cm diameter	Room
6. Deformable surface tubes							
a) GE	5–300 ms	6λ		Yes	Yes		Room
b) IBM (deformographic tube)	20 ms to min		$> 20 \times 10^6$ cycles	Yes	Yes and no	12.5 cm diameter	Room
c) CBS (Lumatron)	20 minutes: < 1 s erase adjustable		$> 3 \times 10^4$ cycles	Yes	Yes	3.8 × 3.8 cm	Room
d) Eidophor				Yes	Yes		Room
7. Ruticon	> 5 ms: 10 ms erasure	$\lambda/4$	$> 10^6$ cycles	Yes	Yes		Room
8. Folded acousto-optic	350 μs	Excellent	∞	Yes (2-D) no (3-D)	Yes	15 cm diameter	Room
9. Membrane light modulator	0.1–1 μs	$\lambda/10$	~ ∞ in vacuum	Yes	Yes	5 mm × 5 mm	Room

	Optical write energy	Electrical write/ maintain energy	Contrast ratio	Resolution	Activation time
1. Liquid crystal light valve	24 ergs/cm² (0.3 ergs/cm² threshold)	Several mW at 10 kHz	> 100:1	> 100 l/mm	10 ms
2. e-Beam KDP (Titus tube)	—	100 μA beam current	60:1	40 l/mm	1/30 s full frame
3. PROM	50 ergs/cm²	4×10^{-4} J/frame	10,000:1	200 l/mm (limiting)	10 ns
4. Photo-Titus (KDP):	100 ergs/cm²	40 W (incl. cooling)	70:1	40 l/mm	10 μs
$(Bi_4Ti_3O_{12})$	2.5×10^{-3} J/cm²		> 100:1	90 l/mm	50 ns
5. Ceramic ferroelectrics (strain biased)	—	50–300 V	< 55:1	30 l/mm	10–50 μs switching
(scattering)	—	50–300 V	1,000:1	40 l/mm	10–50 μs switching
6. Deformable surface tubes					
a) GE	—	1250 W			1 ms
b) IBM (deformographic tube)	—	6×10^{-9} mJ/cm²	> 100:1	15 l/mm	20 ms
c) CBS (Lumatron)	—	7.5 kV		71 l/mm	Few ms
d) Eidophor		20 μA beam current	< 400:1	32 l/mm	< 13 ms
7. Ruticon	10–30 ergs/cm²	300 V bias		> 100 l/mm	< 17 ms
8. Folded acousto-optic	—	Few W		0.5 l/mm	350 μs
9. Membrane light modulator	—	80 V		20 l/mm	0.1–1 μs

Figure 8.1 Characteristics of spatial light modulators (From G R Knight in Lee, see Introduction)

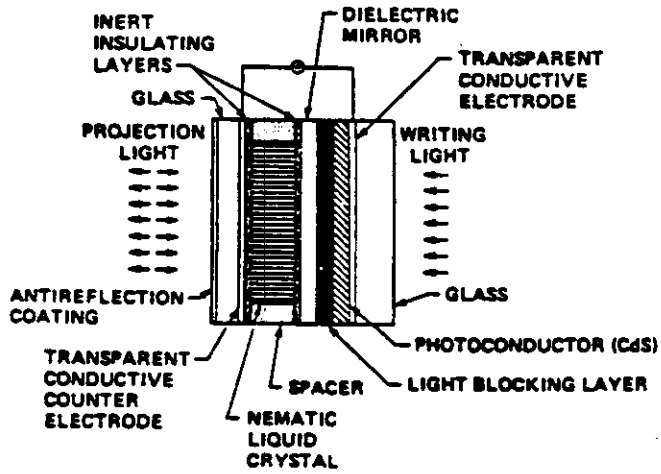

a

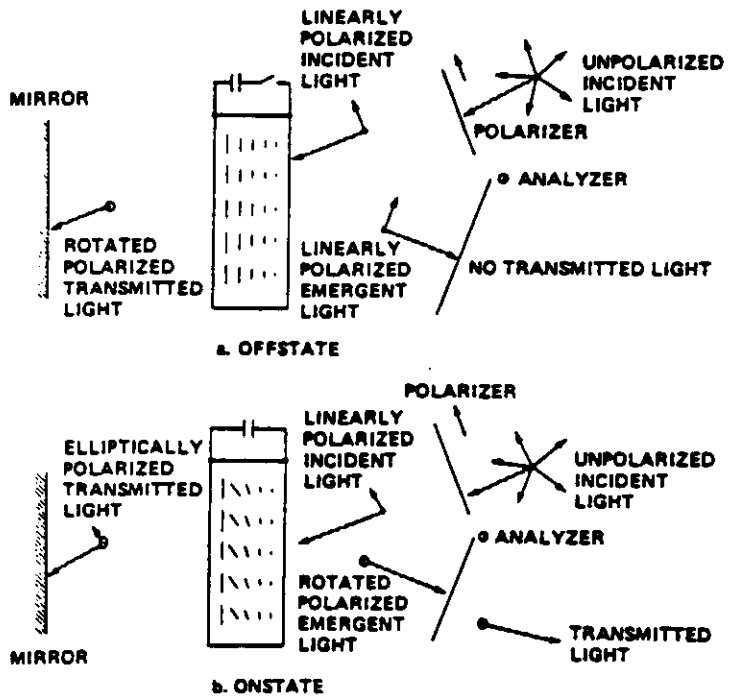

b

Figure 8.2 (a) Schematic diagram of an LCLV
(b) Operation of the device in the off-state (upper) and on-state (lower)
(From G R Knight, in Lee, see Introduction)

The device operates by rotating the plane of polarisation of light and is therefore placed between crossed polarisers in the readout beam as shown in Fig 8.2(b). In the off-state, linearly polarised light is rotated through 45 degrees on its first pass of the layer as a result of the twisted nematic configuration of the crystals but is restored to its original polarisation on the second pass - no light is therefore transmitted by the analyser. In the on-state, with the photoconductor activated, there is a voltage across the liquid crystal layer that causes the molecules to rotate somewhat - the optical birefringence of the layer then causes the plane of polarisation of the twice transmitted light to rotate, thus giving a signal passed by the analyser.

Devices one inch in diameter are available with approximately 1500 resolvable lines across the aperture. The rise time is about 15 ms. In another form of liquid crystal device intended for use as an adaptive Fourier plane filter, electrodes in a ring/wedge matrix modulate the response, thus providing an electronic-to-coherent optical interface.

9. ACOUSTO-OPTIC SIGNAL PROCESSING

9.1 Principles of Operation

Acousto-optical techniques of processing signals utilise either bulk acoustic waves or surface acoustic waves (SAW) (mainly Rayleigh waves). Figure 9.1 illustrates the difference between these two types of waves. In the case of bulk waves, the signal to be analysed is injected by bonding a piezo-electric input plate to the medium (commercial devices have used TeO_2 and $PbMO_4$). In SAW devices, where the acoustic medium (e.g. lithium niobate) is also piezo-electric, use is made of the fact that the surface acoustic wave has an electric field above it in air extending almost one (acoustic) wavelength. The basic SAW element is the delay line, see Fig 9.2(a). The signal is injected using an interdigital transducer which produces an electric field and hence a surface acoustic wave. An interdigital electrode pattern may also be used to detect surface acoustic waves.

For a monochromatic acoustic wave travelling in the z-direction in an isotropic, homogeneous medium, we can represent the refractive index in the region of the wave as

$$n(z,t) = n_0 + n_1 \sin(\omega t - kz) \quad , \qquad (9.1)$$

where n_0 is the unperturbed index and n_1 is the maximum change arising from the sound wave. In the case of SAW, n also varies with depth y into the medium. The velocity of the acoustic wave is typically 10^{-5} that of light, so that an optical beam of free space wavelength λ_{0f} and wavelength λ_0 in the medium sees an almost stationary phase grating of period λ. If the interaction length is small, then the optical beam sees a thin phase grating and is diffracted at angles σ_n,

$$\sin \sigma_n = n\lambda_{0f}/\lambda \quad , \qquad (9.2)$$

with intensity

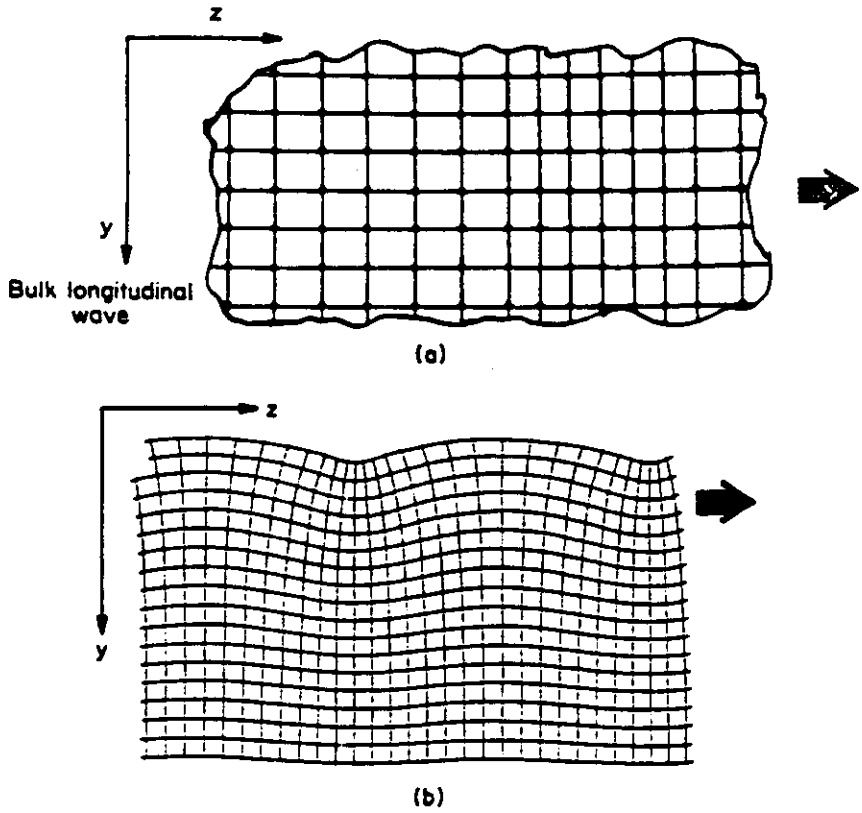

Figure 9.1 Displacements of a rectangular grid in (a) a bulk longitudinal wave (b) SAW (from Das and Ayub, in Stark see Introduction).

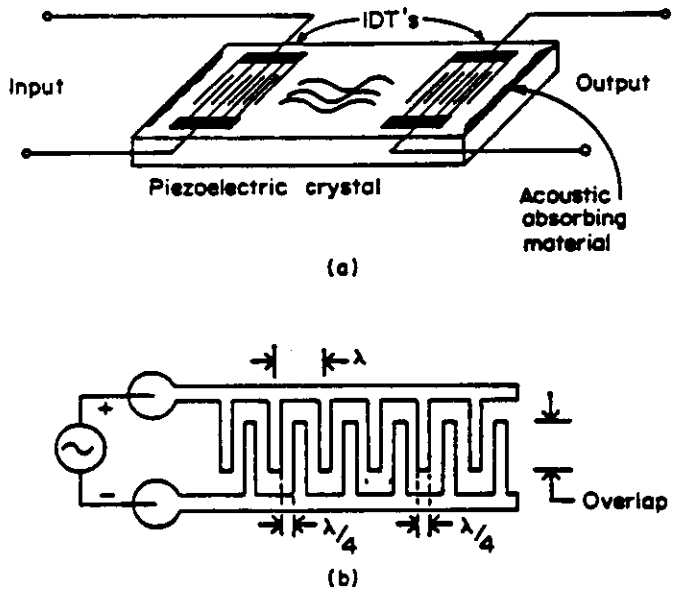

Figure 9.2 (a) SAW delay line (b) interdigital transducer (from Das and Ayub, in Stark, see Introduction).

$$I_n/I = J_n^2(\delta) \quad , \tag{9.3}$$

where

$$\delta = (2\pi/\lambda_0)\, n_1 L$$

and L is the interaction length. The interaction is considered small if $Q \ll 1$, where

$$Q = 2\pi\lambda_{0f} L/(n_0\lambda^2) \tag{9.4}$$

and this type of diffraction is called Raman-Nath diffraction.

If $Q \gg 1$ then Bragg diffraction occurs with a single diffraction angle

$$\sin\sigma_1 = .5\,\lambda_{0f}/\lambda \tag{9.5}$$

of intensity

$$\sin^2(\delta/2) \quad . \tag{9.6}$$

Eq(9.5) can be derived using the usual Bragg diffraction argument or using conservation of momentum between the interacting photons and phonons. Conservation of energy leads to the result

$$\omega_d = \omega_i + \omega_s \tag{9.7}$$

where the suffices d, i and s denote diffracted, incident and sound respectively. Thus the diffracted optical wave is Doppler-shifted in frequency.

Bulk wave acousto-optic devices are commercially available. One key parameter is the time-bandwidth product, $T\Delta f$, where T is the time aperture, i.e. the time taken for an acoustic wave to travel the length of the aperture. A typical TeO_2 modulator has a bandwidth of 30 MHz

centred at 45 MHz, an aperture length of 30 mm or 50μs and a time-bandwidth product of 1500. A $PbMO_4$ device might have a bandwidth of 200 MHz and a time-bandwidth product of 1000. Surface acoustic wave devices are not readily available yet. They can be fabricated as a planar waveguide thus allowing potentially long interaction lengths.

9.2 Applications

Acousto-optic devices can be used as modulators, spectrum analysers, image scanners and convolvers. Fig 9.3 shows a generalised acousto-optic signal processor which can perform all of these operations.

Modulator. With $f_2(t) = 0$ and $T(z) = 1$ in the interval $1/2 < z < 1/2$, the intensity of the diffracted wave can be modulated according to Eq.(9.3) or (9.6) for Raman-Nath or Bragg diffraction respectively.

Spectrum Analyser. With $f_2(t) = 0$, the diffracted light at z' depends on the input frequency of the signal $f_1(t)$. If $f_1(t)$ has many frequencies, a photodiode or charge coupled array in plane z' measures the spectrum of $f_1(t)$.

Image Scanner. With $f_2(t) = 0$, a pulse sent into the acousto-optic device scans the spatial distribution of light $T(\xi)$.

Convolver. Two signals $f_1(t)$ and $f_2(t)$ can be convolved, as shown in Fig 9.4. A review of acousto-optic convolution is given by Rhodes (Proc IEEE, 69, 65-79 (1981)). This convolver can also implement the Fourier transform operation (using a single photodiode, not an array) via the 'chirp' transform algorithm: the Fourier transform (see Eq.1.1) may be written

$$F(\omega) = \exp(-\pi i\omega^2) \int_{-\infty}^{\infty} \{f(t) \exp(-\pi i t^2)\} \exp[\pi i(t-\omega)^2]\, dt \qquad (9.8)$$

This is equivalent to multiplying the original signal by a chirp $\exp[-\pi i t^2]$, convolution with a chirp $\exp[-\pi i t^2]$ and then multiplication

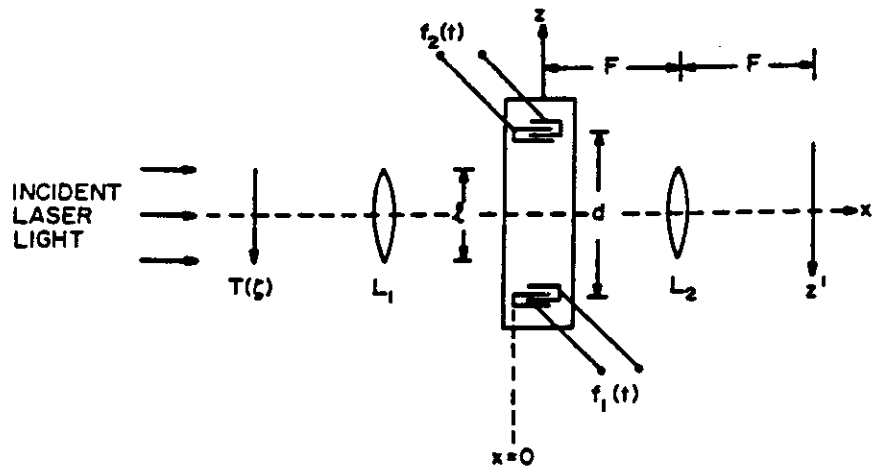

Figure 9.3 Generalised acousto-optic signal processor (From Das and Ayub, in Stark, see Introduction).

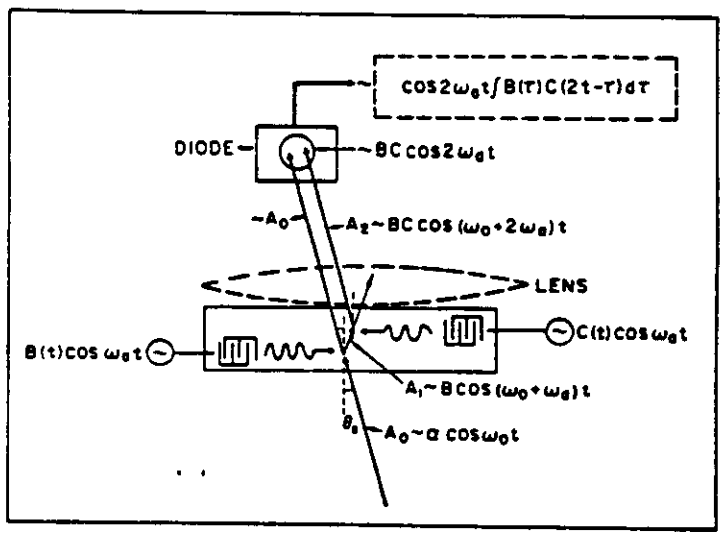

Figure 9.4 Signal convolution using acousto-optic interaction (From Berg et al, Opt Engng 19, 359-369 (1980)

by the chirp $\exp[-\pi i\omega^2]$.

All of the above functions can in principle be carried out in a planar waveguide using surface acoustic waves. Fig 9.5 shows the design of a spectrum analyser in a planar waveguide.

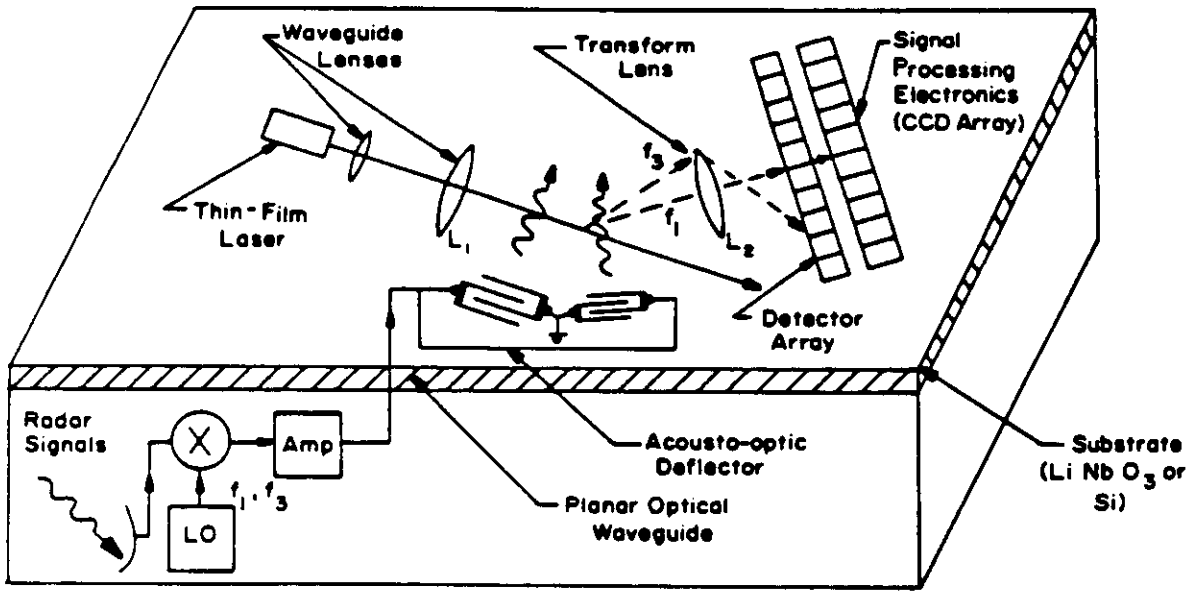

Figure 9.5 Schematic of an integrated acousto-optic rf spectrum analyser (after Tsai et al, Proc SPIE, 154, 60-63 (1980)).

10. NON-COHERENT OPTICAL PROCESSING

10.1 Introduction

All of the optical information processing techniques that have been described so far rely on the fact that the light is monochromatic and spatially coherent (i.e. there is a fixed phase relationship between all spatial points). Such radiation is naturally emitted by most lasers. However, it is well-known that coherent illumination gives rise to spurious fringing effects when dust or other optical imperfections are present in the optical system. Furthermore, any randomly rough surface gives rise to laser speckle which severely degrades the quality of images formed in perfectly coherent light. (Laser speckle is discussed in the Statistical Optics lectures).

Light that is either temporally non-coherent (i.e. polychromatic), and/or spatially non-coherent (i.e. emanating from an extended source) reduces these artifacts by an amount depending on its degree of coherence. Totally incoherent light does not give rise to any speckle at all.

In this Section we present a few simple examples of non-coherent optical processing. Further details may be found in the books by Lee, Rogers, Stark and Yu (see Introduction). Methods of non-coherent processing can be conveniently classified into those that are based on the wave nature of light and those based essentially on geometrical optics. We describe polychromatic spatially coherent and monochromatic spatially incoherent optical Fourier transform systems as examples of the former and two Fourier transform systems based on geometrical optics as examples of the latter. However, it should be stressed that many other optical processing operations other than the Fourier transform can be carried out by non-coherent optical systems.

10.2 The Achromatic Optical Fourier Transform

In Section 2.1 we stated that the complex amplitude in a Fraunhofer diffraction pattern was given by

$$U(x,y) = \frac{-i}{\lambda}\frac{\exp(ikz)}{z}\exp\left[\frac{ik(x^2+y^2)}{2z}\right] \iint_{-\infty}^{\infty} U(\xi,\eta)\exp\left[\frac{-2\pi i}{\lambda z}(x\xi+y\eta)\right] d\xi\, d\eta. \quad (2.1)$$

This is the complex amplitude at a large distance from a coherently illuminated diffracting screen. As shown in Section 2.1, a lens can be used to achieve an exact Fourier transform relationship between its front and back focal planes, with distances (x,y) in the Fourier plane being related to spatial frequencies (u,v) of the input plane by

$$x = \lambda f u \quad \text{and} \quad y = \lambda f v .$$

Suppose now that an input object, for example a grating of frequency (u,v), is illuminated by spatially coherent but <u>polychromatic</u> (white light). This could be achieved by replacing the laser source with a small tungsten-halogen lamp. Each wavelength λ in the illumination will now form a pair of diffraction spots at $(\lambda fu, \lambda fv)$ resulting in a pair of <u>spectra</u> in the back focal plane.

An achromatic Fourier transform optical system is one which compresses the spectra back to small spots, i.e. gives a relationship

$$x = \bar{\lambda} f u \quad \text{and} \quad y = \bar{\lambda} f v ,$$

where $\bar{\lambda}$ is a pre-determined constant. Such optical systems can be designed using at least two separated lens groups, as shown by Wynne (Opt Commun <u>28</u>, 21-26 (1979)) and Morris (Appl Optics <u>20</u>, 2017-2025 (1981)).

Figure 10.1 shows the effect of using an achromatic Fourier transform lens when the object consists of a set of nested triangles. By using two achromatic Fourier optical systems in tandem one can construct an achromatic matched filtering or inverse filtering optical processor.

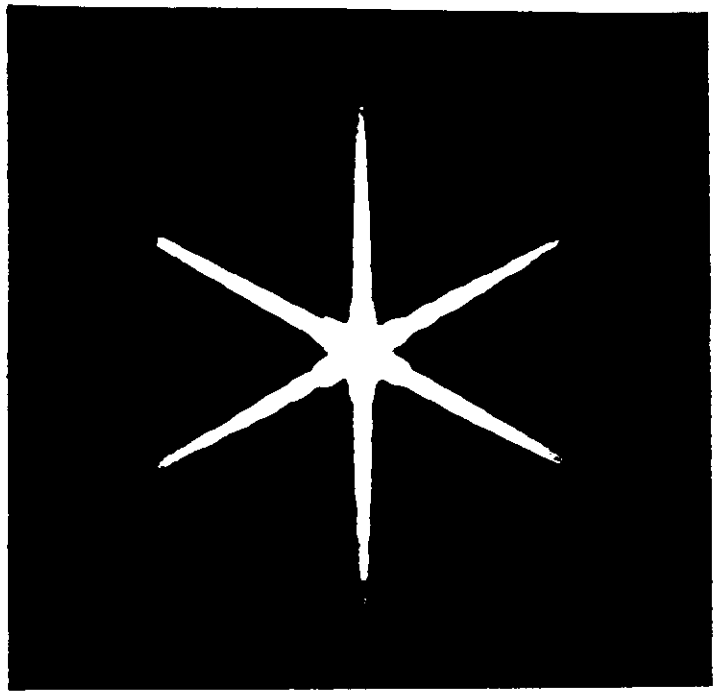

a

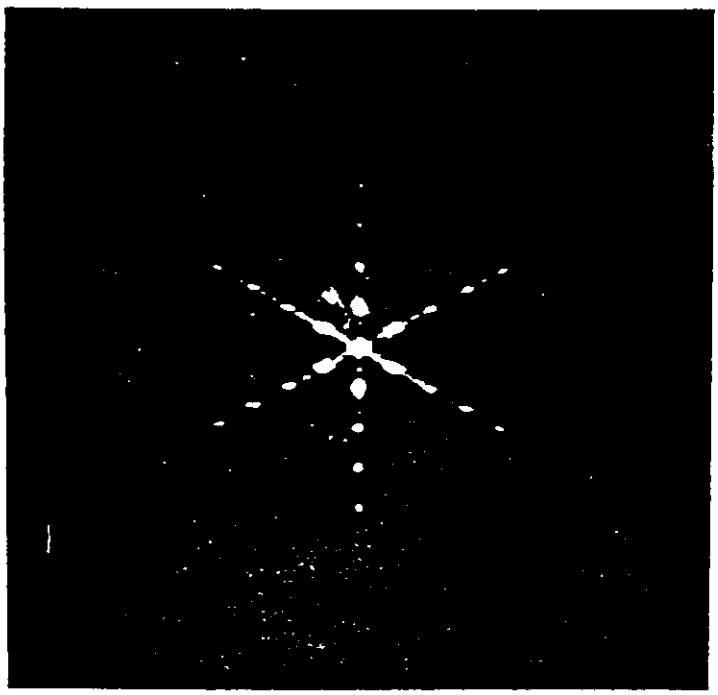

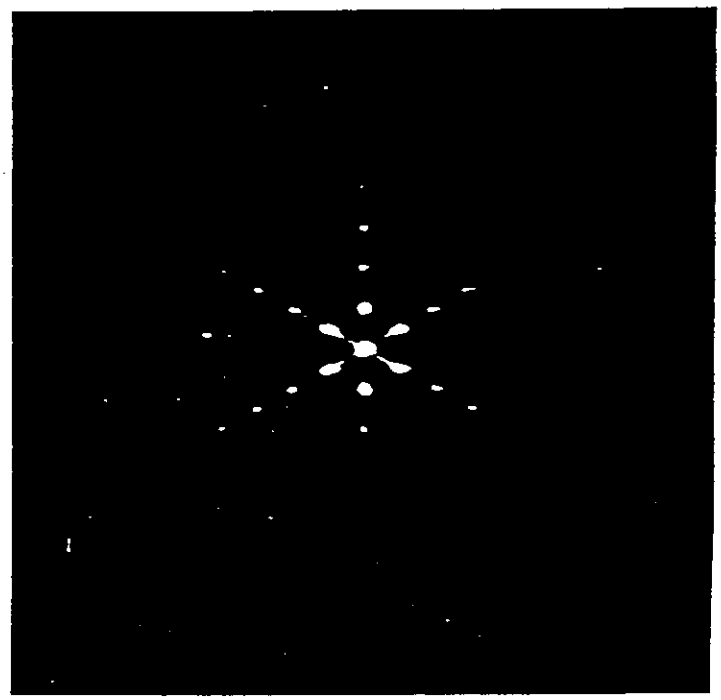

b

Figure 10.1 (a) Output of a conventional coherent diffractometer for an input consisting of nested triangles illuminated by white light.
(b) Output of achromatic diffractometer (left $\Delta\lambda$=300nm, right $\Delta\lambda$=200 nm).
(Courtesy of G M Morris and N George)

10.3 Monochromatic Spatially Incoherent Fourier Tansforms

Suppose that we wish to optically find the Fourier transform of a spatially incoherent distribution of light, such as a transparency illuminated by an extended source or a television monitor. We shall assume here that the light is fairly monochromatic, although the technique described below can be made achromatic.

Let the light intensity of the object whose Fourier transform is to be found be denoted by $I(\xi,\eta)$ and the time-varying complex amplitude incident upon a distant detector be $V(x,y,t)$. In coherent light, $V(x,y,t)$ would be a well-behaved sinusoidally varying signal, but in incoherent thermal (chaotic) light it is a randomly varying function. However, as shown by van Cittert and Zernike (see Born and Wolf, 'Principles of Optics, Pergamon Press, 6th Ed, 1980), the statistical correlation or mutual intensity of $V(x,y,t)$ is equal to the Fourier transform of $I(\xi,\eta)$, provided certain elementary conditions are satisfied. Thus, defining the mutual intensity

$$M(x,y) = \langle V(x',y',t)\ V^*(x'+x,y'+y,t)\rangle \qquad (10.2)$$

then the van Cittert-Zernike theorem gives,

$$M(x,y) = \iint_{-\infty}^{\infty} I(\xi,\eta)\ \exp\left[\frac{-2\pi i}{\lambda z}(x\xi+y\eta)\right]\ d\xi\ d\eta \qquad (10.3)$$

where z is the (large) distance from the source plane (ξ,η) to the observation plane (x,y).

Any technique of measuring the mutual intensity thus also measures the Fourier transform of the intensity distribution $I(\xi,\eta)$. The simplest way of measuring $M(x,y)$ is to use an interferometer - we shall describe a one-dimensional interferometer, but it can easily be extended to two dimensions (see Mertz, 'Transformations in Optics', Wiley, 1965, Breckinridge, Applied Optics, 13, 2760-2762 (1974) and Roddier et al, J Optics (Paris), 9, 145-149 (1978)).

The wavefront-folding interferometer (see Fig 10.2) gives an intensity at its output equal to

$$I(x,y) = \langle | V(x,t) + V(-x,t) |^2 \rangle$$

$$= 2 [1 + \mathrm{Re}\{M(2x,0)\}] \qquad (10.4)$$

if the intensity $|V|^2$ is spatially uniform and set equal to unity for normalisation. Since $I(\xi,\eta)$ is necessarily real, it follows that $\mathrm{Re}\{M(2x,0)\}$ is equal to a section of the Fourier cosine transform of $I(\xi,\eta)$. The Fourier sine transform can be measured by introducing an additional $\pi/2$ phase change in one arm, for example, by translating the mirror by $\lambda/8$.

10.4 Fourier Transforms using Geometrical Optics

One simple non-coherent method of Fourier transformation is based on the use of Moire fringes. Fringes of cosinusoidal (or sinusoidal) intensity distribution of frequency (u,v) illuminate a transparency $t(\xi,\eta)$. If all of the transmitted light is collected by a detector, the detector output is proportional to the cosine (sine) transform of $T(\xi,\eta)$ at spatial frequency (u,v). This is a very simple way of finding the Fourier transform, although like most non-coherent methods it suffers from the presence of a large DC component in the measurements.

The incoherent optical system shown in Fig 10.3(a) can be used to perform the following matrix operation

$$[g] = [S]\,[f] \qquad (10.5)$$

and a discrete Fourier transform is a special case of this. This system can of course only deal with real, positive light intensities. However, as shown by Goodman et al (Opt Lett 2, 1-3 (1978)) complex signals can be handled by decomposing them into three components - this means that for N complex input points we require 3N real inputs (light emitting diodes), a 3N x 3N mask and 3N outputs (photo-diodes).

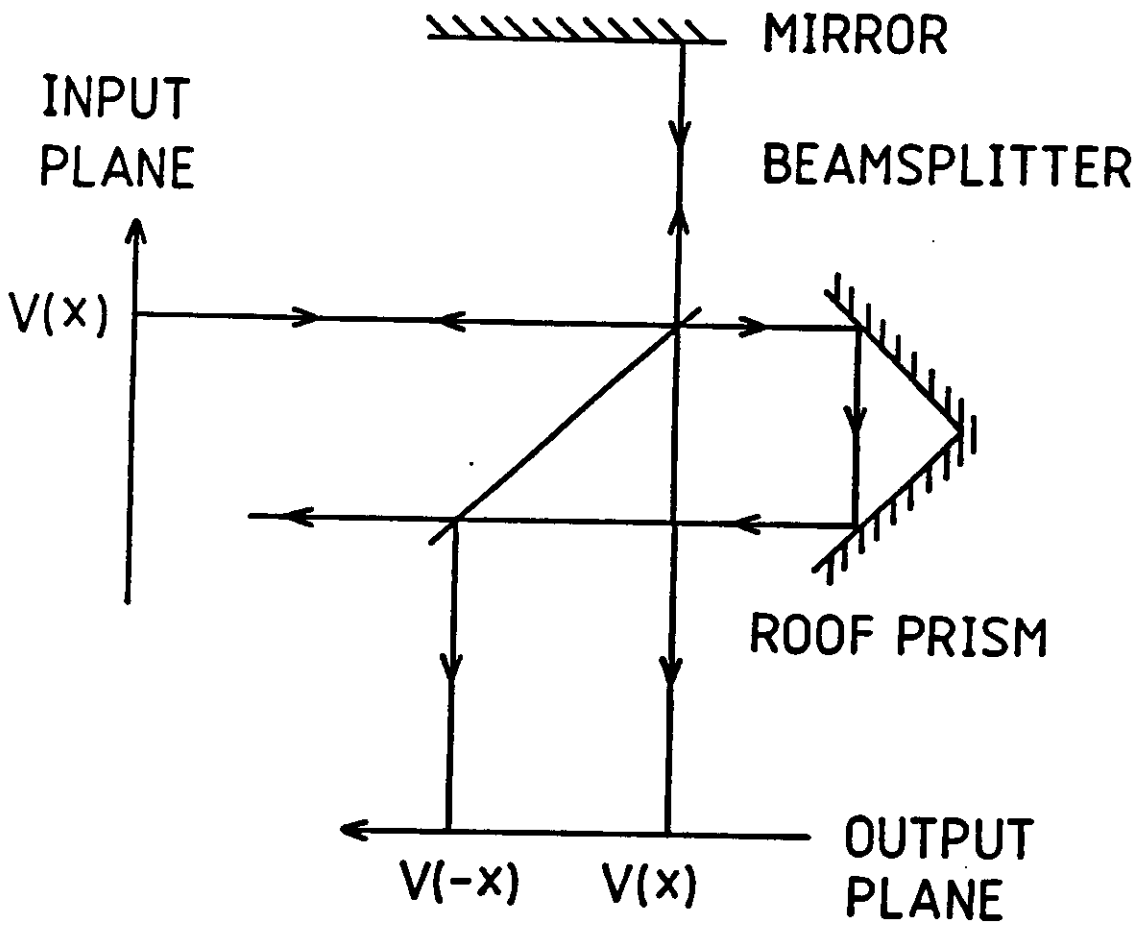

Figure 10.2 The wavefront-folding interferometer

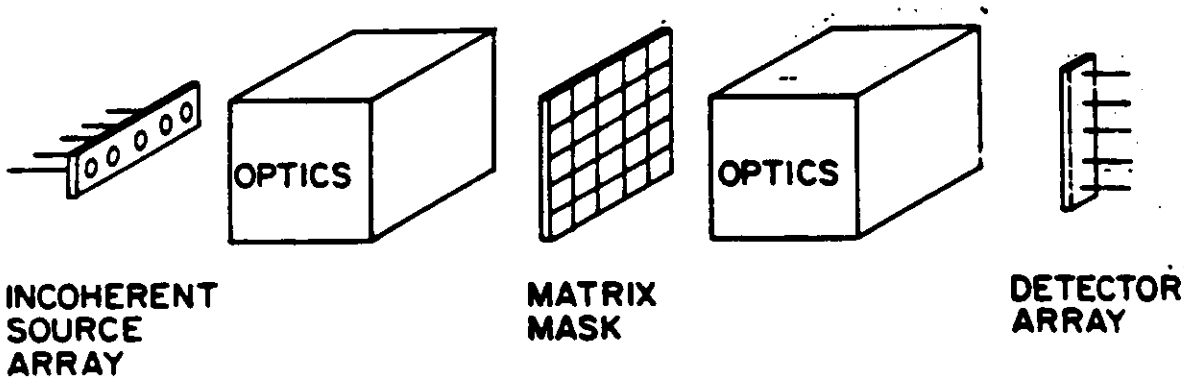

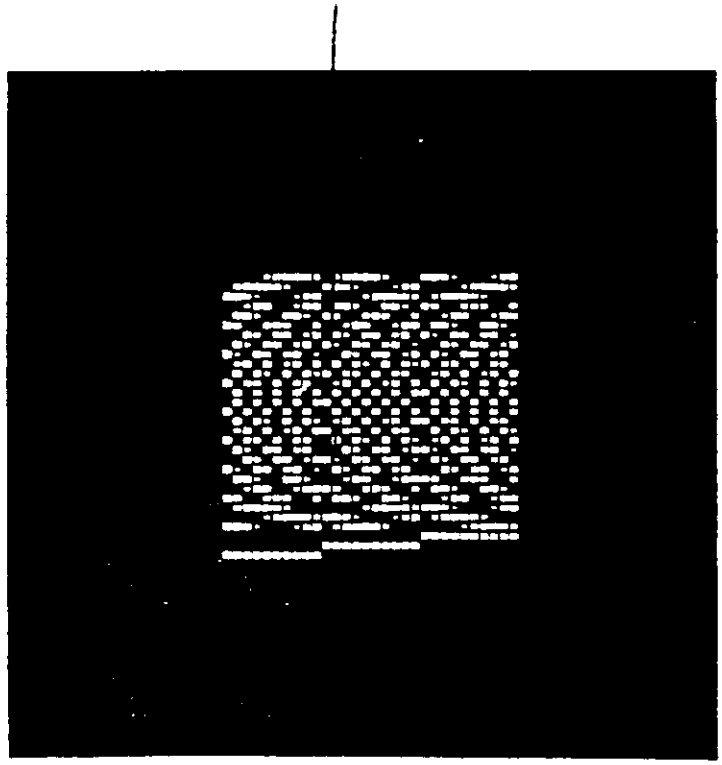

Figure 10.3 Basic incoherent system for matrix-vector multiplication (after Goodman et al, Opt Lett 2, 1-3 (1978))